Case study regarding the energy efficiency of a modular house having ecological envelope

Studiu de caz privind eficiența energetică a unei case modulare cu anvelopa ecologică

Georgiana Corsiuc[1], Carmen Mârza[2].

[1]Universitatea Tehnică din Cluj-Napoca, Facultatea de Instalații
B-dul 21 Decembrie 1989, nr. 128-130, Cluj Napoca, România
E-mail: georgiana@mail.utcluj.ro

[2] Universitatea Tehnică din Cluj-Napoca, Facultatea de Instalații
B-dul 21 Decembrie 1989, nr. 128-130, Cluj Napoca, România
E-mail: carmen.marza@insta.utcluj.ro

Abstract. *In this paper, the authors propose a case study on the energy efficiency of a house built in accordance with sustainable development directions. Thus, the envelope is made of ecological materials, namely the resistance structure and finishes are made of wood, and the thermal insulation of sheep's wool. It is a modular, prefabricated house, designed so that energy consumption is reduced both in the construction and exploitation phase. Having a built area of 31.5 m², it can be used as a residential house or a holiday home. For this, the thermotechnical properties of the envelope elements were studied.*

Key words: ecological construction, energy efficiency, envelope structure, thermal resistance, heat transfer coefficient, thermal stability, water vapor permeability.

1. Introduction

Two of the fundamental challenges of our times, namely the energy and the environment, significantly concern the field of civil engineering.

In the last few years, one has faced the pandemic problem caused by Sars Cov 19 which has changed people's mentality and generated their desire to "migrate" from crowded urban areas to more isolated areas, which was possible due to the work and education in the online system, through various platforms. On the other hand, the energy problem that has been in the attention of society since the last decades of the 20th century, has become acute nowadays due to the political situation created by the conflict generated by the Russian Federation, which represented an important supplier of fossil fuels for many states in the Union European and beyond. In this complicated context, a significant number of people have chosen to ensure alternative residences. A practical solution is represented by modular houses - as a quick construction method, which must

be as ecological as possible, energy efficient and having independence from the centralized energy system if the energy is provided from renewable sources.

As it is known, an ecological house can be defined synthetically, as a house built and exploited with a lot of responsibility towards the environment, during its entire life cycle, starting with the design phase, then construction, maintenance, renovation, including also the demolition phase [1].

As a result of global statistics, yields that about 40% of the total energy consumption is due to constructions, including the construction itself and its exploatation, so that the microclimate conditions required by the occupants are ensured.

Regarding the heat losses through the envelope, results that these have the following structure: about 35% through the walls, 30% through the roofs, 20% through the glazed surfaces, respectively 15% through the floors. Although this information are relative, it is useful to have an overview of the selection of materials and solutions related to the elements of the envelope, having the main goal to improve the energy performance of buildings [2].

Considering the previous information, the authors proposed a solution for the construction of a modular house, made of ecological materials and carried out a study regarding the thermotechnical properties of the envelope elements, respectively for the external walls and for the covering. Moreover, the use of wood in the construction of residential houses is recommended on the one hand due to the creation of a healthy microclimate in the homes, and on the other hand due to the low thermal conductivity coefficient, which is approximately 7-10 times higher than to concrete, respectively 3-4 times compared to brick [3].

2. Presentation of the proposed house and analysis of thermotechnical properties

2.1. The plan of the house and the main hygrothermal properties

The modular house proposed to the beneficiaries considered their requests regarding the dimensions, partitioning, construction materials and obviously the costs. The envelope plays an important role in achieving and maintaining the comfort conditions for a construction in the general way and implicitly in the case of ecological houses. In short, it separates the heated volumes of the construction from the external environment and from other elements characterized by different temperatures, which are in contact with it [4]. Fig. 1 presents the floor plan of the house, having a constructed area of 31.5 m^2.

In fact, the house was designed at the request of some beneficiaries from a rural, semi-montane area in Austria, having a placement similar to climate zone III in our country, i.e., the exterior temperature of -18 ºC. For these conditions, the verification of the requirements related to the hygrotemic behavior of the envelope elements was carried out using the Ubakus U-value calculator [5].

Following, are presented the measurements that are automatically calculated, obviously according to the proposed structure for the elements.

Thus, related to thermal protection, the following physical quantities are obtained:

- specific thermal resistance R [m^{2}K/W] → defines the property of the materials through which the heat is transferred to oppose the propagation of heat losses; in the case of a construction element consisting of several homogeneous layers, it represents the sum of the convective resistances of the fluid media (air) in the vicinity of the element and the actual conductive resistance of the element [4], [6];
- heat transfer coefficient (or transmittance) [W/m^{2}K], represents the reverse of the thermal resistance; it reflects the heat transfer capacity, so the lower the U value is, the lower the transmission losses are [4], [6];
- temperature variation within the structure of the envelope elements and the surface temperatures, which gives an image of heat losses and reflects the possibility of condensation risk of [6], [7].
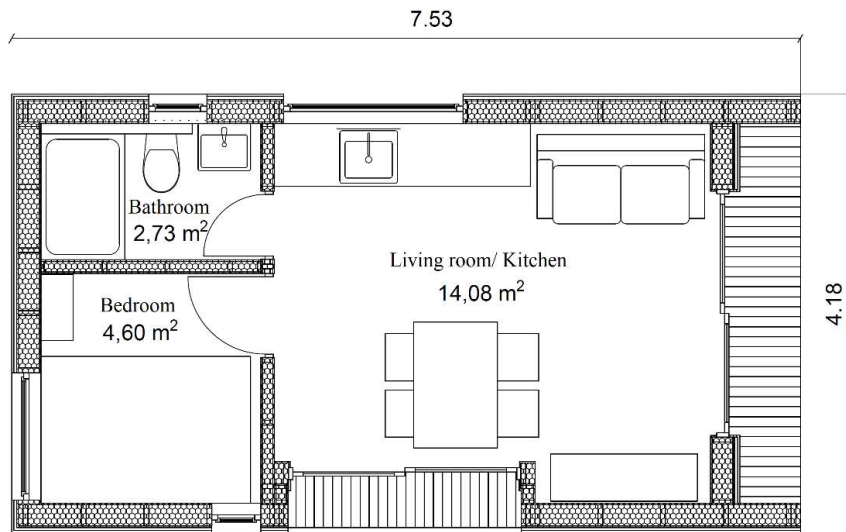
Fig. 1. The floor plan of the modular ecological house

An important interest and facility that this program provides are related to the thermal stability of the closing elements and not of the rooms as whole. The thermal stability of buildings represents their ability to maintain the amplitudes of the variations of the indoor air temperature and the temperatures of the interior surfaces of the elements within the admissible limits, required by the compliance of the indoor thermal comfort conditions [4], [6], [7].

Thus, depending on the layers that build up the closing element, it results:
- The phase shift coefficient, represents the time in hours after which the temperature peak of the afternoon reaches the component interior and has usually values between 6 and 14 hours, depending on the thermotechnical properties of the materials [4], [6], [7];
- The amplitude attenuation coefficient of the outdoor air oscillation, which is defined as the ratio between the outdoor air temperature oscillation amplitude and the temperature oscillation amplitude it determines on the inner surface of

the building element; it is dimensionless, and it is recommended to be contained within the range 16 … 25 [4], [6], [7].

These coefficients are also normed in Romanian standards.

The Ubakus program implicitly calculates other quantities, such as the temperature amplitude - as the reverse of the previous coefficient, the heat storage capacity, the thermal capacity of the inner layers, etc. [5].

From the point of view of the vapor permeability of the envelope elements, the Ubakus calculation program provides graphs that show how the relative humidity varies in the wall structure [5]. It also implicitly calculates a quantity **Sd**, which represents the vapor diffusion resistance of the construction elements, which the Romanian standards did not provide in this form. This represents the equivalent thickness of the air layer to the diffusion of water vapor, and is calculated with the formula:

$$Sd = \mu_x\, d \;[m] \qquad\qquad (1),$$

where, μ= vapor diffusion resistance coefficient, depending on the material,

d= the thickness of the material layer subjected to vapor transition [m].

The lower the value, the less resistance the building element opposes and allows vapor to diffuse more easily.

2.2. Exterior walls

In the following, the thermotechnical properties that the Ubakus application [5] generates, depending on the structure proposed by the authors, are presented, namely:

• Figure 2 shows the constructive structure of the external walls;

• a section through the wall is shown in Figure 3;

• Figure 4 shows the oscillation of the surface temperature during one day and the phase shift of the heat wave propagation;

• Figure 5 shows the variation of relative humidity in the wall structure.

thermo-treated pine (20 x 80)
wooden support batten (27 x 50)
spruce (200 x 45)
sheep wool thermal insulation (200 mm)
vapor barrier membrane
wooden support batten (20 x 45)
plywood (16 mm)
OSB (15 mm)
highly breathable monolithic membrane
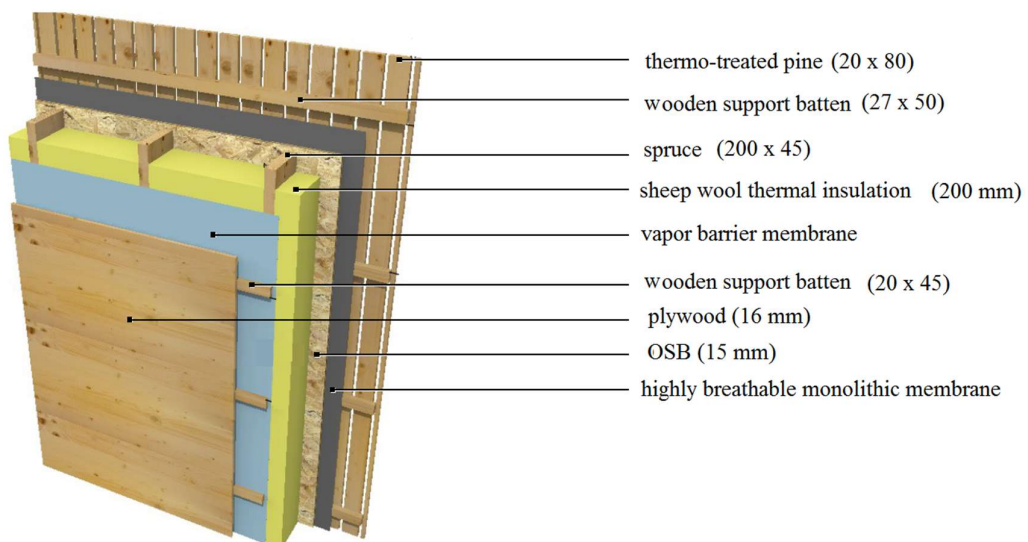
Fig.2. The constructive structure of the external walls

Case study regarding the energy efficiency of a modular house having ecological envelope
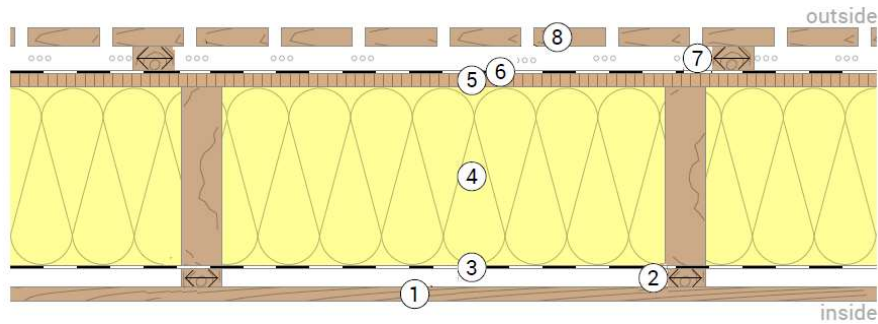
Fig.3. Section through the exterior wall

1. Plywood; 2. Wooden support batten; 3. Vapor barrier membrane; 4. Sheep wool thermal insulation; 5. OSB board; 6. Highly breathable monolithic membrane resistant to uv rays; 7. Wooden support batten; 8. Thermo-treated pine facade.
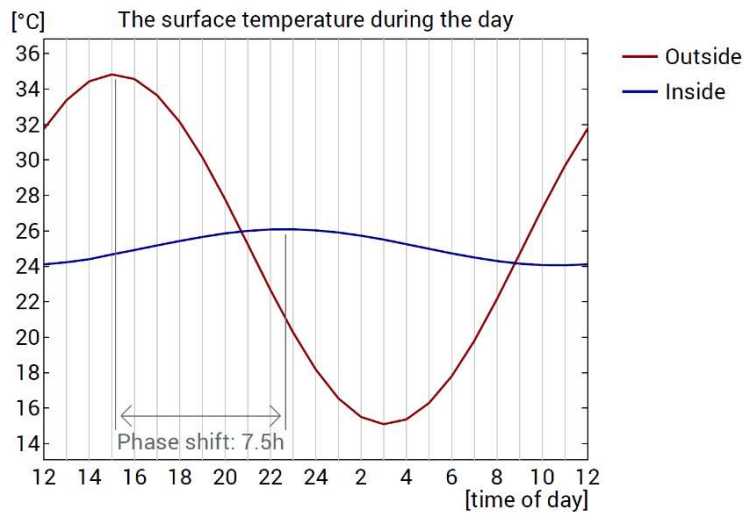
Fig.4. The surface temperature during the day
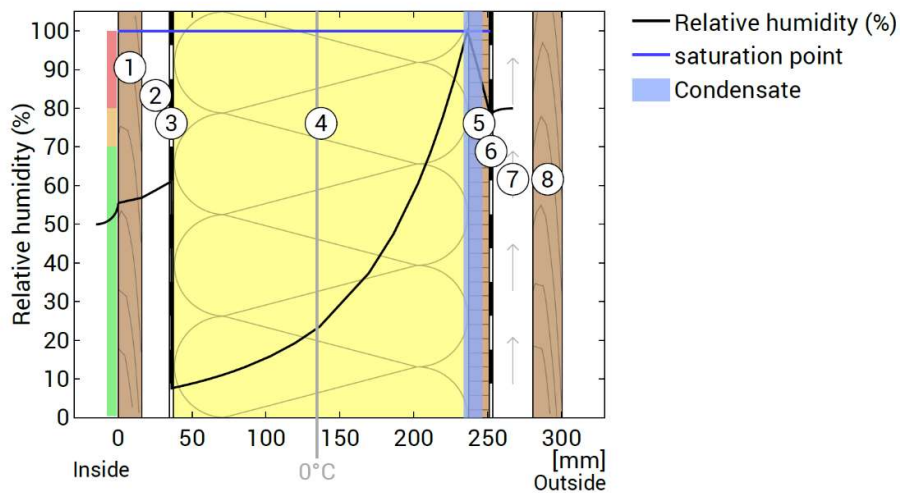
Fig.5. The relative humidity inside the component

Table 1 shows the physical dimensions that characterize the thermal protection of the external wall components. In addition, the program directly calculates the heat transfer coefficient of the external wall, i.e. U = 0.2 W/m2K. This value complies with the recommendations of the ISO standard [8], being close to the requirements imposed on an energy-efficient house.

Table 1

The hygrothermal properties of the external wall components

Material	Thickness [cm]	Thermal conductivity [W/mK]	Thermal resistances [m2K/W]	Sd-value [m]
Thermal contact resistance (Rsi)			0.130	
Plywood	1.60	0.160	0.100	0.80
Stationary air	2.00	0.114	0.175	0.01
Wooden support batten (8.3%)	2.00	0.130	0.154	
Vapor barrier membrane	0.02	0.400	0.001	40.00
Sheep wool thermal insulation	20.00	0.039	5.195	0.20
Wooden support batten (8.3%)	20.00	0.130	1.538	4.00
OSB board	1.50	0.130	0.115	3.00
Highly breathable monolithic membrane	0.1	0.200	0.005	0.10
Thermal contact resistance (Rse)			0.040	
Whole component	29.17		5.03	

2.3. The roof

As in the case of the walls, the thermotechnical characteristics of the covering that the Ubakus application [5] generates, depending on the structure proposed by the authors, are presented, namely:

- Figure 6 shows the construction elements of the covering;
- Figure 7 shows a section through the covering;
- Figure 8 shows the oscillation of the surface temperature during one day and the phase shift of the heat wave propagation;
- Figure 9 shows the variation of relative humidity in the structure of the covering.
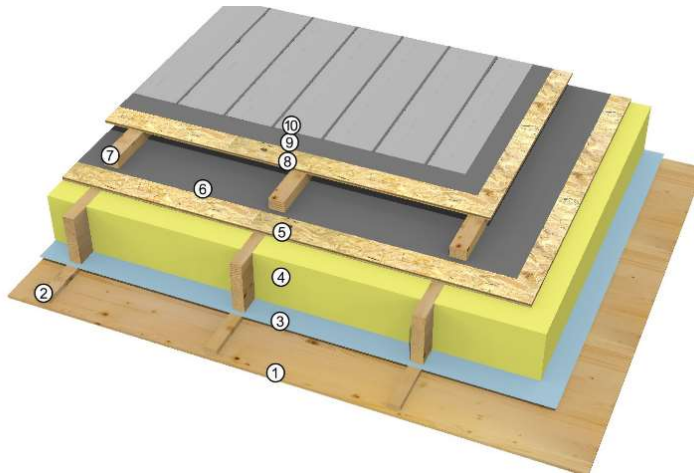
Fig.6. The constructive structure of the covering
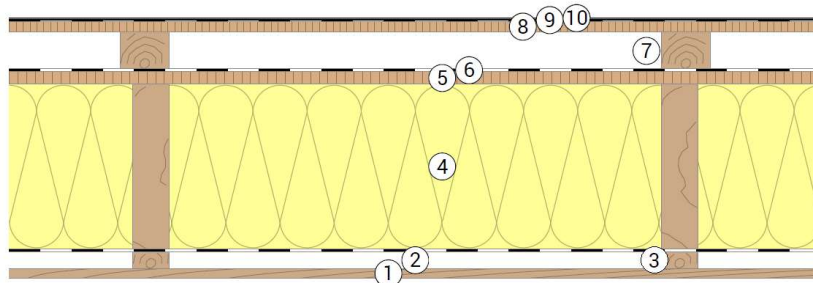
Fig.7. Section through the roof

1.Plywood; 2. Wooden support batten; 3. Vapor barrier membrane; 4. Sheep wool thermal insulation; 5. OSB board; 6. Highly breathable monolithic membrane resistant to uv rays; 7. Wooden support batten; 8. OSB board; 9. Highly breathable monolithic membrane resistant to uv rays; 10.Metal sheet.
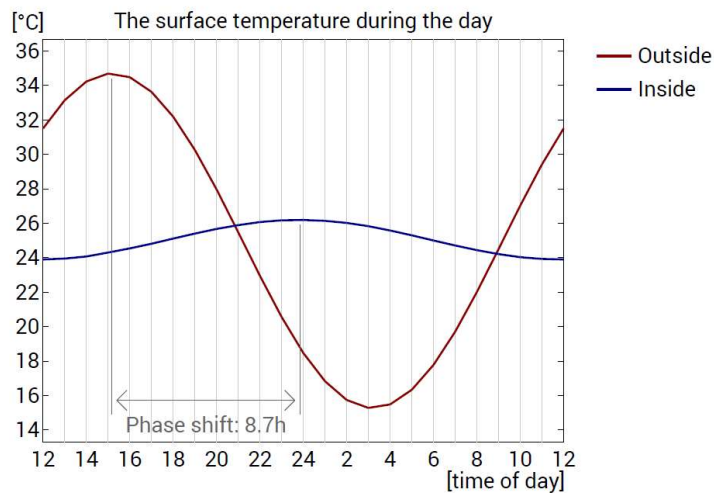
Fig.8. The surface temperature during the day
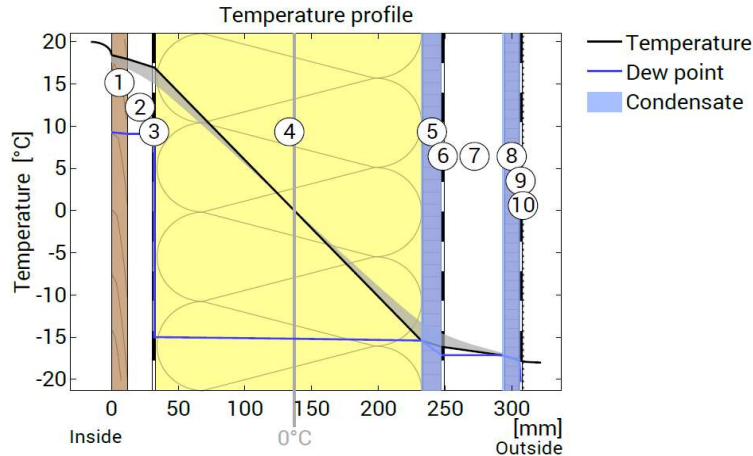
Fig.9. The relative humidity inside the component

Table 2 shows the physical quantities that characterize the thermal protection of the component elements of the covering. Once more, the program directly calculates the heat transfer coefficient, namely U = 0.19 W/m2K. With these values, the chosen solution falls within the norms agreed in Austria [8].

Table 2

The hygrothermal properties of the component elements in the envelope

| Material	Thickness [cm]	Thermal conductivity [W/mK]	Thermal resistances [m2K/W]	Sd-value [m]
Thermal contact resistance (Rsi)			0.100	
Plywood	1.20	0.160	0.075	0.60
Stationary air	2.00	0.125	0.160	0.01
Wooden support batten (7%)	2.00	0.130	0.154	0.80
Vapor barrier membrane	0.02	0.400	0.001	40.00
Sheep wool thermal insulation	20.00	0.039	5.195	0.20
Wooden support batten (7%)	20.00	0.130	1.538	4.00
OSB board	1.50	0.130	0.115	3.00
Highly breathable monolithic membrane	0.07	0.300	0.002	0.02
Stationary air	4.5	0.281	0.160	0.01
Wooden support batten (9.1%)	4.5	0.130	0.346	1.8
OSB board	1.20	0.130	0.0.92	2.40
Highly breathable monolithic membrane	0.07	0.300	0.002	0.02
Metal sheet	0.10	10.000	0.000	1500
Thermal contact resistance (Rse)			0.040	
Whole component	30.66		5.32	

3. Conclusions

In this paper, the authors proposed and presented, structures for the envelope elements - external walls and covering, to meet as many requirements and demands as possible, among which we briefly mention the most important ones:
• to have good hygrothermal properties, i.e. to ensure good thermal protection, thermal stability of the closing elements, appropriate vapor permeability behavior, without

allowing the accumulation of water in the structure of the envelope elements;
• to be constructed quickly, to be transportable by road – the house having the destination in Austria, to have an acceptable weight, to be easy to assemble and handle; obviously, wooden constructions are very suitable for these requirements;
• to use environmentally friendly materials that can be recycled or reused.

In this sense, one mention the use of wood as the main construction material and sheep's wool, for thermal insulation respects the requirements of an ecological house. Wool must be pre-treated for pest protection with urea derivatives, and for fire and mold protection with boron salts. However, its special thermotechnical properties especially recommend it, even if other solutions could generate lower costs.

Finally, in Figure 10 are given photos of the studied house.

Fig.10. Photos of the studied house

References

[1] G. Corsiuc, C. Mârza, Case study regarding the energy efficiency of green buildings envelope, Revista Romana de Inginerie Civila, Volumul 11 (2020), Numărul 1, pp. 17-24.
[2] C. Mârza, G. Corsiuc, Aspecte privind structura pereților exteriori a clădirilor verzi (Aspects regarding the exterior wall structure for green buildings), Volumul Conferinței „Instalații pentru începutul mileniului trei", Sinaia, 12-14 oct 2016, Ed. Matrix Rom, pp. 298-307.
[3] Constantin Miron, Livia Miron, Construcții din lemn adaptate cerințelor uniunii europene pentru 2020 (Wooden constructions adapted to the requirements of the European Union for 2020), Buletinul Institutului de Cercetări Științifice în Construcții, Nr.6-CI, 2015, pp. 41-53.
[4] C. Mârza, A. Abrudan, Elemente de termotehnica construcțiilor (Elements of building thermotechnics), U.T.Press, Cluj-Napoca, 2012.
[5] ***C107-2005 Normativ privind calculul termotehnic al elementelor de construcție ale clădirilor (Normative regarding thermotechnical calculation of construction elements of buildings).
[6] E. Comsa, I. Moga, C. Munteanu, Proiectarea higrotermica si auditul energetic al anvelopei cladirilor civile (Hygrothermal design and energy audit of the envelope of civil buildings), U.T. Press, Cluj Napoca, 2010.
[7] https://www.ubakus.com/en/r-value-calculator/
[8] ***ISO 6946:2017 Building components and building elements — Thermal resistance and thermal transmittance.

High-strength cellular building material prepared by direct microwave heating using industrial silicate wastes and borax

Material de construcție celular cu înaltă rezistență produs prin încălzire directă cu microunde utilizând deșeuri silicatice industriale și borax

Lucian Păunescu[1], Sorin-Mircea Axinte[2,3], Bogdan-Valentin Păunescu[4]

[1] Cosfel Actual SRL
95-97 Calea Grivitei street, M4 room, sector 1, Bucharest 010705, Romania
E-mail: lucianpaunescu16@gmail.com

[2] Daily Sourcing & Research SRL
95-97 Calea Grivitei street, sector 1, Bucharest 010705, Romania
E-mail: sorinaxinte@yahoo.com

[3] Department of Applied Chemistry and Material Science, University „Politehnica" of Bucharest
1-7 Gh. Polizu street, sector 1, Bucharest 011061, Romania
E-mail: sorinaxinte@yahoo.com

[4] Consitrans SA
56 Polona street, sector 1, Bucharest 010504, Romania
E-mail: pnscbogdan@yahoo.com

Rezumat. *Vitroceramica celulară a fost produsă prin sinterizare la 850-860 ℃ utilizând, ca materie primă principală, cenuşă zburatoare de cărbune (74-79 %), un produs secundar industrial, borax (20-25 %), ca agent de fluidizare și carbonat de calciu (1 %), ca agent de spumare clasic. Originalitatea lucrării a fost aplicarea tehnicii neconvenționale, rapidă și economică, a încălzirii directe cu microunde. Această tehnică nu este utilizată în procese similare industriale. Rezultatele au arătat rezistență foarte mare la compresiune (11,7-18,3 MPa), proprietăți termoizolante bune, adecvate pentru aplicații in construcție și consum specific de energie foarte redus (0,50-0,60 kWh/kg).*

Cuvinte cheie: vitroceramică celulară, încălzire directă cu microunde, cenuşă zburătoare de cărbune, borax, rezistență la compresiune.

Abstract. *Cellular glass-ceramic was produced by sintering at 850-860 ℃ using, as the main raw material, coal fly ash (74-79 %), an industrial by-product, borax (20-25 %,) as a fluxing agent and calcium carbonate (1 %), as a classic expanding agent. The originality of the work was the application of the unconventional, fast and economical technique of direct microwave heating. This technique is not used in similar industrial*

processes. The results showed very high compressive strength (11.7-18.3 MPa), good thermal insulation properties, suitable for building applications and very low specific energy consumption (0.50-0.60 kWh/kg).

1. Introduction

The global energy and ecological crisis that appeared at the end of the 20th century caused major changes in all spheres of economic activity affected by the need to reduce energy consumption by recycling industrial waste or from other types of activities.

For a long time, recycling waste resulting from the demolition or redevelopment of buildings was not a common practice. There was an exception at the end of World War II in several European countries (Germany, UK, etc.) due to the huge quantities of masonry rubble available for the manufacture of aggregates for new constructions [1, 2]. The global concern has resurfaced in recent decades with the need to reduce energy consumption for the manufacture of common building materials and reduce greenhouse gas emissions. Currently, the annual rate of masonry rubble generation is 70 million tons in the UK and 50-60 million tons in Germany [3].

Building materials containing wastes of concrete, clay brick, natural aggregate, and other mineral components were used for manufacturing lightweight aggregate [4]. The raw material was crushed, ground in a ball mill, pelletized in a disc pelletizer, fired and stabilized in a rotary kiln. Silicon carbide as an expanding material was added. The sintering temperature was 1160-1180 ºC obtained by conventional heating process. Pellets with dimensions between 2-8 mm, bulk density between 0.7-1.0 g cm^{-3}, compressive strength between 4-5 MPa, and water absorption in the range 8-15.5 vol. % were obtained at the end of process.

Another recipe for the manufacture of lightweight aggregates based on clay brick, mortar, plaster, lightweight, aerated, and normal concretes, and sand lime brick is presented in [5]. Raw material was crushed, ground, and sieved, the grain size being sub 100 μm. The adopted pore-supplying agent was silicon carbide (SiC) in a weight ratio of 3 %. The mixture was pelletized in a disc pelletizer and then conventionally heated in a rotary kiln to the optimum temperature for maximum material expansion of 1185 ºC. In terms of quality, the lightweight aggregate produced from masonry rubble was almost similar to that of lightweight expanded clay aggregate (LECA).

The processes of manufacturing porous materials (cellular glass-ceramics) using silicate industrial waste or industrial by-products, other than recycled glass waste, have facilitated applying the unconventional technique of direct microwave heating. Previous experiments performed by the Romanian company Daily Sourcing & Research SRL showed that glass (soda-lime glass type) is not suitable for direct microwave irradiation at the usual frequency of 2.45 GHz and specific powers between 1.50-1.65 kW/kg (typical for the microwave oven commonly used in the household and also in experiments presented in the literature [6-9]). The direct irradiation causes the destruction of the macrostructure of glass in its core at the

foaming temperature. Instead, the silicate industrial waste, even with glass waste, but in very low proportions, subjected to the direct microwave heating at very high rates are not structurally affected. This experimental finding allowed to successfully carry out foaming the building waste and the manufacture of cellular glass-ceramic with thermal insulation properties and high compressive strength.

According to the paper [6], experiments aiming at the manufacture by direct microwave heating of a high-strength aggregate included in the raw material composition clay waste from construction (70.5-83.4 %), coal fly ash (9 %), colored glass waste (2.6-15.5 %), SiC (5 %) as a pore-supplying agent, and water (20-28 %) as a binder. The temperature of the sintering process was between 1055-1150 ºC reached in 24-32 min due to the very high heating rate (35.3-43.1 ºC/min). The thermal insulation properties of the cellular glass-ceramic (apparent density between 0.60-0.69 g cm^{-3} and heat conductivity between 0.100-0.116 W (mK)$^{-1}$) were satisfactory and the compressive strength had high values (7.8-8.3 MPa). The water absorption was within normal limits (9.3-17.5 vol. %) taking into account that the starting material contained a high percentage of clay.

Aggregate made only from clay waste (75-83 %) and coal ash (15-23 %) as raw material, SiC (2 %) as a pore-supplying agent and water (25 %) as a binder by sintering at 1115-1145 ºC in a microwave oven by direct irradiation [7] led to the production of a material with properties suitable for high-strength aggregate having the apparent density between 0.50-0.68 g cm^{-3}, heat conductivity in the range 0.078-0.095 W (mK)$^{-1}$, compressive strength between 3.8-7.5 MPa, water absorption between 11.9-12.8 vol. %, and pores with high dimensions (up to 2.5 mm), reaching even 5 mm in the case of variant that used the maximum proportion of coal ash.

Aggregate manufacturing recipe including masonry rubble (85.6-90.8 %) and coal ash (4-9 %) as raw material, SiC (3.5-5.5 %) as a pore-supplying agent, and water (18 %) as a binder was applied in [3], the direct irradiation heating at 1168-1185 ºC with very high heating rates between 33.9-35.9 ºC/min leading to products with an apparent density between 0.75-0.98 g cm^{-3}, heat conductivity between 0.123-0.140 W (mK)$^{-1}$, compressive strength between 6.0-7.3 MPa, and coarser porosity with pore size between 1.2-4.5 mm.

Other work [8] using masonry rubble (88.5-93.0 %) and coal fly ash (4-7 %) as raw material, SiC (3.0-4.5 %) as a pore-supplying agent and water addition (18 %) as a binder applied the same technique of direct microwave heating at 1160-1170 ºC, the heating rate varying between 34.0-38.5 ºC/min. The thermal insulation properties of the specimens were better than the paper [3], the apparent density being between 0.40-0.54 g cm^{-3}, the thermal conductivity between 0.079-0.096 W (mK)$^{-1}$, and the porosity between 74.3-81.0 %, while the compressive strength had high values (5.5-7.0 MPa). Pore size was low reaching a maximum of 1.5 mm.

Work [9] using clay brick from demolished building waste (78.5-84.6 %) and clear residual flat glass (9.4-15.5 %) as raw material, borax (4 %) as a fluxing agent, SiC (2 %) as a pore-supplying agent, and water addition (15 %) as a binder presents a technique of manufacturing the high-strength aggregate by direct microwave

irradiation, reaching high heating rates (34.0-42.4 ºC/min). The sintering and foaming temperature range was 1080-1143 ºC. The thermal insulation properties indicated a denser material: apparent density between 0.72-0.98 g cm^{-3}, porosity between 53.3-65.7 %, and thermal conductivity in the range 0.161-0.197 W (mK)$^{-1}$. The compressive strength reached high values between 6.4-8.5 MPa. Pore size was low, the maximum value reaching 1.1 mm.

Very high mechanical strength cellular glass-ceramic was manufactured by direct microwave heating at 853 ºC using very high weight ratio of coal fly ash (82 %), calcium carbonate (5 %) as an expanding agent, sodium carbonate (13 %) as a fluxing agent, and water addition (10 %) as a binder [10]. The thermal insulation properties had high values (apparent density of 1.44 g cm^{-3} and heat conductivity of 0.281 W (mK)$^{-1}$), while the compressive strength reached a very high value (41.3 MPa). The application domain of this porous glass-ceramic may include construction types that require high mechanical stress (road and railway construction, bridge abutments, foundations, drainages, sports grounds, etc.).

Recent work [11] has highlighted a new technique for the manufacture of cellular glass-ceramic by the direct overfiring of coal fly ash at relatively low temperature due to the addition of borax without the use of a usual pore-supplying agent. When the critical point of the densification temperature is exceeded, the glass-ceramic foam porosity increases and the pore dimension also increases, being the basis of the porous glass-ceramic manufacture by direct overfiring. By adding borax the boron-oxygen bond can change the structure of quartz and the network of amorphous vitreous phase in coal fly ash. According to [12], self-expansion of coal fly ash could occur at the sintering temperature, crystals being able to precipitate in molten to form pores. The experimental results showed that the overfiring temperature of coal ash has a high value (about 1190 ºC). The use of borax as a fluxing agent was the solution adopted for the significant decrease of the process temperature. The above-mentioned work [11] used coal fly ash/borax mixtures in ratios from 90/10 to 70/30. The borax proportion influenced bulk density, porosity, and flexural strength values. It has been experimentally found that with the increase of borax addition and process temperature, the viscosity of vitreous phase and the bulk density gradually decrease and the porosity gradually increases. Borax ratio of 15 % led to the temperature decrease to 1000 ºC, the 20 % ratio allowed the temperature decrease to 925 ºC, while the 25 % ratio allowed reaching the low temperature of 822 ºC.

In view of the previous experimental results exposed above, the present work aimed to produce by sintering at a relatively low temperature a porous glass-ceramic material using coal fly ash, borax as a fluxing agent and calcium carbonate (CaCO$_3$) as a pore-supplying agent under the conditions of applying the unconventional microwave fast heating technique. The originality of the work is the use of the unconventional technique of direct microwave heating, practically not applied in the world in cellular glass-ceramic manufacturing processes and to a very small extent previously tested by the authors of this paper.

2. Materials and methods

The main raw material used in this experiment was coal fly ash, an industrial by-product of the thermal power stations. The material has been provided by the Paroseni station from Romania having the following chemical composition: 46.5 % SiO_2, 23.7 % Al_2O_3, 7.9 % CaO, 3.2 % MgO, 6.0 % Na_2O, 4.1 % K_2O, 8.2 % Fe_2O_3, and 0.4 % other oxides. The coal ash has been taken over with the grain size below 250 μm and has been mechanically processed in an electric grinding device up to grain dimensions below 100 μm.

Because Na_2O is known as an excellent fluxing material and sodium tetraborate decahydrate ($Na_2B_4O_7 \cdot 10H_2O$), known as borax, contains 30.8 % Na_2O [13, 14], this material was adopted as a fluxing agent in experiments. Also, its high ratio of boron in the form of B_2O_3 creates the borax ability to significantly increase the mechanical strength of the expanded product. Borax was purchased from the market as a crystalline white powder.

Calcium carbonate ($CaCO_3$) one of the most effective pore-making agents having a fine grain size (below 5 μm) has been also used in the starting mixture.

The adopted method was mainly based on the ability of coal fly ash to expand itself by the liquid-phase direct sintering process forming numerous pores in the molten material mixture including borax to decrease the process temperature due to its fluxing property. The addition of $CaCO_3$ as a pore-supplying agent contributes to the foaming process. $CaCO_3$ decomposes in the temperature range 750-900 ºC releasing CO_2 as gas bubbles [15-17] according to reaction (1), which are blocked in the molten and turn in a pore network after cooling.

$$CaCO_3 = CaO + CO_2 \qquad (1)$$
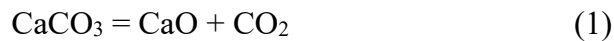
The equipment used in this experiment was a 0.8 kW-microwave oven of the household type for food preparation, but constructively adapted for operation at much higher temperatures (up to 1200 ºC). The direct microwave heating of the pressed powder mixture applied in this experiment has a special peculiarity by comparison with the conventional heating processes. The unconventional heating is initiated in the core of the irradiated material, where the microwave power is converted into heat. Thus, the highest temperature level is reached in the middle of the material and the propagation of heat takes place volumetrically from inside to outside [18, 19], i.e. inversely to its propagation in conventional techniques. Under these conditions, the thermal protection of the irradiated material with 1200 ºC-resistant ceramic fiber mattresses is essential. Although the metal walls of the microwave oven were not protected, the heat loss outside was kept low (below 70 ºC) despite the very high temperature of the thermal process (around 1000 ºC). Pyrovar-radiation pyrometer mounted above the oven in its central axis allowed monitoring the evolution of the temperature of irradiated material by viewing it through 30 mm-holes provided in the upper metal wall of the oven and in the ceramic fiber mattress that protects the upper

area of the hot material. The constructive and functional scheme of the experimental equipment is shown in Fig. 1.
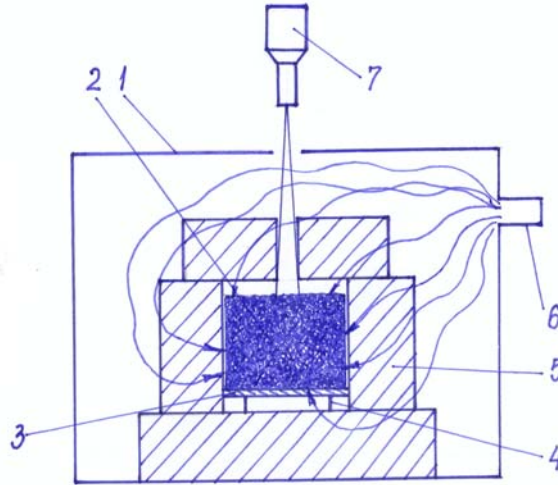
Fig. 1. Constructive and functional scheme of the experimental equipment
1 – microwave oven; 2 – pressed powder mixture; 3 – metal plate; 4 – metal support;
5 – ceramic fiber heat protection; 6 – waveguide; 7 – radiation pyrometer.

The following methods were applied to characterize the cellular glass-ceramic specimens. The gravimetric method [20] was used to determine the apparent density and the method of comparing the "true" density and the apparent density [21] was used to calculate the porosity of the specimens. Determining the heat conductivity was performed by heat-flow method (ISO 9869-1: 2014, reviewed and confirmed in 2019) and the TA.XTplus Texture analyzer was used to identify the compressive strength (EN 826-2013). To measure the volumetric proportion of absorbed water in the material it was applied the method of specimen immersion in water (for 24 hours) (ASTM D570). The microstructural peculiarities of cellular glass-ceramic specimens were examined with ASONA 100X Zoom Smartphone Digital Microscope. To identify the crystalline phases of the porous materials, the XRD technique (EN 13925-2:2003) was applied using X-ray diffractometer Bruker-AXS D8 Advance with CuKα radiation.

3. Results and discussion

Four experimental variants containing coal fly ash, borax, $CaCO_3$, and water addition as a binder were adopted to test manufacturing the high-strength cellular glass-ceramic. The $CaCO_3$ weight proportion was kept constant at 1.0 %, while coal ash/borax ratio was modified from 87/12 up to 74/25. The composition of experimental variants is shown in Table 1.

Table 1

Composition of experimental variants

Variant	Coal fly ash (wt. %)	Borax (wt. %)	$CaCO_3$ (wt. %)	Water addition (wt. %)
1	87.0	12.0	1.0	10.0
2	83.0	16.0	1.0	10.0
3	79.0	20.0	1.0	10.0
4	74.0	25.0	1.0	10.0

The main functional parameters of the sintering/expanding process are presented in Table 2.

Table 2

Functional parameters of the heat process

Parameter	Variant 1	Variant 2	Variant 3	Variant 4
Dry raw material/cellular glass-ceramic amount (g)	430/ 418.6	430/ 419.0	430/ 418.7	430/ 418.5
Sintering/foaming temperature (ºC)	830	840	850	860
Heating time (min)	20	21	22	24
Average rate (ºC/min) · heating · cooling	40.5 5.3	39.0 5.4	37.7 5.2	35.0 5.4
Index of volume growth	1.30	1.45	1.60	1.85
Specific energy consumption (kWh/kg)	0.50	0.52	0.55	0.60

According to the data in Table 2, constant amount (430 g) of solid starting material was used in this experiment. The method consisted in simultaneous increase of the weight ratio of borax (Table 1) and heating temperature from 830 to 860 ºC. The exceptional energy efficiency of the heating process by direct microwave irradiation of the pressed material led to very short durations (20-24 min) and heating rates between 35.0-40.5 ºC/min, much higher compared to the rates commonly used in conventional processes [15]. The volume of irradiated material has increased by foaming the coal ash powder and forming the pore network by 30-85 %. Variant 1 with 12 % borax and the process temperature of 830 ºC produced a dense structure, while variant 4 with 25 % borax simultaneously with reaching the temperature of 860 ºC generated a porous structure with larger pore dimensions. In terms of energy, the manufacturing process of cellular glass-ceramic using coal fly ash as the main raw material, borax, and $CaCO_3$ were extremely economical in all four variants, the specific energy consumption values being very low (0.50-0.60 kWh/kg) at a lower level compared to the most efficient industrial processes.

Images of the cross section-appearance of cellular glass-ceramic specimens are shown in Fig. 2.
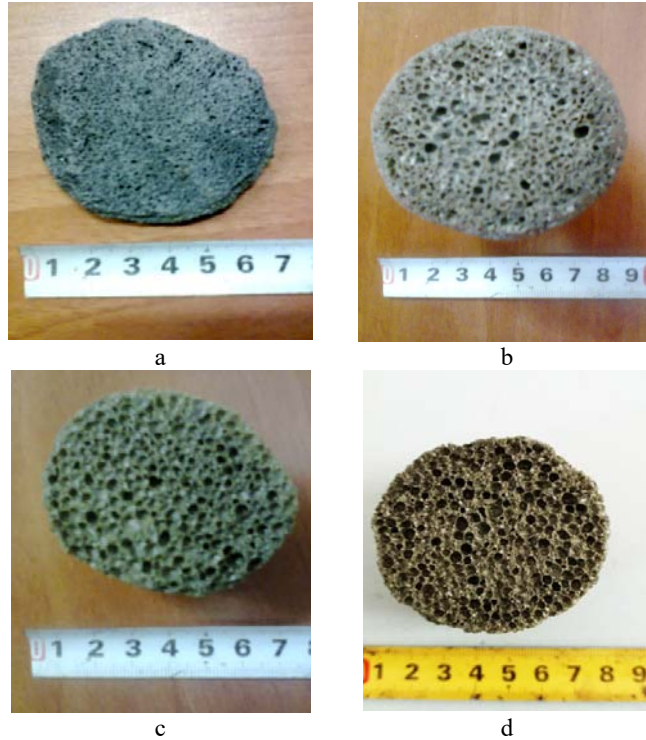
Fig. 2. Cross section-appearance of specimens
a – specimen 1 heated at 830 ºC; b – specimen 2 heated at 840 ºC;
c – specimen 3 heated at 850 ºC; d – specimen 4 heated at 860 ºC.

The physical, thermal, mechanical, and morphological characteristics of specimens determined by the analysis methods mentioned above are indicated in Table 3.

Table 3

Physical, thermal, mechanical, and morphological features

Variant	Apparent density (g cm^{-3})	Porosity (%)	Heat conductivity [W (mK)$^{-1}$]	Compressive strength (MPa)	Water absorption (vol. %)	Pore size (mm)
1	1.10	47.6	0.228	29.7	1.2	0.15-0.50
2	0.96	54.3	0.198	23.0	1.1	0.25-0.65
3	0.80	61.9	0.172	18.3	0.9	0.40-1.00
4	0.65	69.0	0.140	11.7	0.7	0.60-1.20

The data in Table 3 show remarkable mechanical features, the specimen compressive strength being in the range 11.7-29.7 MPa. Unfortunately, the thermal insulation properties of the material are affected especially in the case of variants 1 and 2, which due to the dense character of their macrostructure have high values of apparent density (0.96-1.10 g cm^{-3}) and heat conductivity [0.198-0228 W (mK)$^{-1}$] as

well as quite low values of porosity (47.6-54.3 %). The values of the physical-thermal characteristics that define the thermal insulation properties of specimens 3 and 4 (density between 0.65-0.80 g cm^{-3}, heat conductivity between 0.140-0.172 W (mK)$^{-1}$, and porosity between 61.9-69.0 %) are acceptable. These physical-thermal characteristics together with the compressive strength values and the low level of water absorption (below 0.9 vol. %) constitute excellent performances of cellular glass-ceramic materials made by the technology presented in this work.

The microstructural homogeneity of specimens, shown in Fig. 3, is also a physical feature favourable for the thermal insulator role of the material.
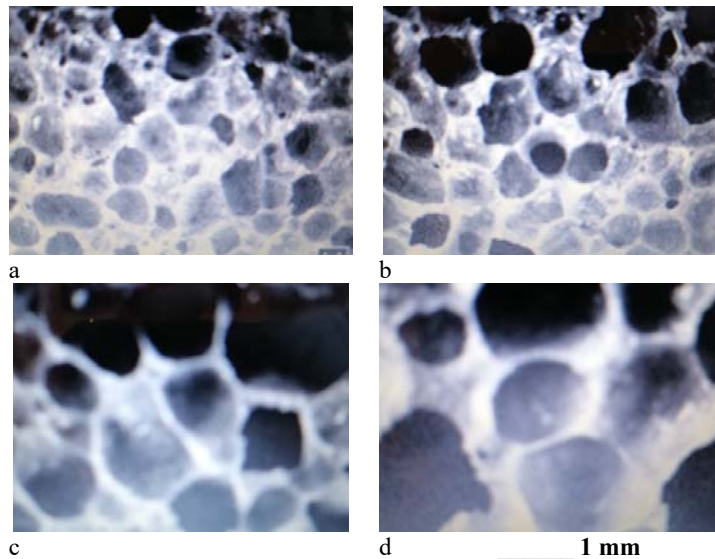
Fig. 3. Microstructural appearance of cellular glass-ceramic specimens
a – specimen 1; b – specimen 2; c – specimen 3; d – specimen 4.

According to the pictures in Fig. 3, the pore size varied between the four experimental variants. With the increase of the weight proportion of borax and the process temperature, the pore size increased, reaching in variant 4 the range of values 0.60-1.20 mm. The other ranges of values corresponding to variants 1-3 are indicated in Table 3.

According to [22], glass-ceramics are fine microstructure-materials containing at least one crystalline phase making by the controlled crystallization. Various silicate-based wastes such as coal ash, metallurgical slag, fly ash and filter dusts from waste incinerators, red mud from zinc hydrometallurgy, sludges, etc. are adequate for production of glass-ceramics. The crystalline phases of the cellular glass-ceramic manufactured in this experiment were identified by the XRD technique. It has been observed that proportions of borax between 12-20 % lead to obtaining specimens having as main crystalline phase quartz and to a lesser extent anorthite and mullite. In the case of specimen 4 with 25 % borax, practically the only crystalline phase identified was quartz.

Manufacturing recipe of cellular glass-ceramic adopted by authors replaced recycled glass waste with an industrial by-product (coal fly ash) resulting as a residue from coal burning in thermal power stations. Coal fly ash has the ability to expand itself at the sintering temperature, borax significantly reducing the melting temperature. $CaCO_3$ as an usual expanding agent was supplementary used contributing also to pores forming. Applying this recipe had as a result manufacturing porous product with high compressive strength. On the other hand, the making process of this type of material made by rapid and economical unconventional direct microwave heating allowed to reach excessively high heating rates, well above the limit recommended in the literature (10-15 ºC/min) [15], without affecting the microstructural homogeneity of the product. It should be mentioned that the direct microwave heating which in the case of using glass waste as a raw material was not suitable, being instead perfectly adequate in the case of other industrial silicate waste (e.g. coal ash) [23].

4. Conclusions

The current work aimed at the experimental manufacture of cellular glass-ceramic using coal fly ash, an industrial by-product, as the main raw material, borax as a fluxing agent, and calcium carbonate (1 %) as a classic expanding agent. The replacement of recycled glass waste commonly used as silicate waste with coal ash was based on its ability to expand itself at the sintering temperature, significantly reduced due to the addition of borax (between 12-25 %). The originality of the paper was applying the unconventional technique of direct microwave heating not used in industrial processes, where less fast and less economical conventional methods are preferred. The method consisted in simultaneous increasing the weight ratio of borax and heating temperature from 830 to 860 ºC. The exceptional energy efficiency of the heating process by direct microwave irradiation of the pressed material led to heating rates between 35.0-40.5 ºC/min, much higher compared to the rates commonly used in conventional processes. Of the four variants tested, the variants prepared from 20-25 % borax, 74-79 % coal ash, 1 % $CaCO_3$, and 10 % water addition were considered optimal, the mixture being sintered at 850-860 ºC. The results indicated very high compressive strength (11.7-18.3 MPa) and good thermal insulation properties (apparent density of 0.65-0.80 g cm^{-3}, heat conductivity of 0.140-0.172 W (mK)$^{-1}$, porosity of 61.9-69.0 %) suitable for use as thermal insulation material in construction domains that require high resistance to mechanical stress. The specific energy consumption values were very low (0.50-0.60 kWh/kg) at a lower level compared to the most efficient industrial processes.

References

[1] F.M. Khalaf, A.S. DeVenny, „Recycling of demolished masonry rubble as coarse aggregate in concrete: Review", Journal of Materials in Civil Engineering, vol. 16, no. 4, 2004. https://doi.org/10.1016/(ASCE)0899-1561(2004)16:4(331)

[2] A.S. DeVenny, „Recycling of demolished masonry rubble", PhD Thesis presented at Napier University of Edinburgh, Scotland, UK, October 1999.

[3] L. Paunescu, M.F. Dragoescu, S.M. Axinte, Ana C, Sebe, „Lightweight aggregate from recycled masonry rubble achieved in microwave field", Nonconventional Technologies Review, vol. 23, no. 2, 2019, pp. 47-51.

[4] A. Moeller, A. Schnell, K. Ruebner, „The manufacture of lightweight aggregates from recycled masonry rubble", Construction and Building Materials, vol. 98, 2015, pp. 376-387. https://www.elsevier.com/locate/conbuildmat

[5] Petra Jakubcová, D. Adomat, P. Ramge, K. Rübner, „New lightweight aggregates from building waste", European Coatings Journal, vol. 2, 2011, pp. 35-39.

[6] L. Paunescu, M.F. Dragoescu, Felicia Cosmulescu, „Microwave heat treatment of wastes (clay, glass and coal ash) to manufacture a high mechanical strength cellular aggregate", Nonconventional Technologies Review, vol. 24, no. 4, 2020, pp. 64-71.

[7] L. Paunescu, M.F. Dragoescu, S.M. Axinte, „Thermal insulating material with high mechanical strength made from clay brick waste and coal ash using the microwave energy", Journal of Engineering Studies and Research, vol. 26, no. 2, 2020, pp. 28-34.

[8] L. Paunescu, S.M. Axinte, Felicia Cosmulescu, „Recycled masonry rubble used as raw material for manufacturing lightweight aggregate by an unconventional heating method", The Bulletin of Polytechnic Institute from Iasi-Chemistry and Chemical Engineering Section, vol. 67 (71), no. 4, 2021, pp. 51-62.

[9] L. Paunescu, M.F. Dragoescu, S.M. Axinte, Felicia Cosmulescu, „Nonconventional manufacture technique of cellular glass from recycled aluminosilicate glass-based waste", Material Science & Engineering International Journal, vol. 5, no. 1, 2021, pp. 11-16.

[10] L. Paunescu, S.M. Axinte, M.F. Dragoescu, Felicia Cosmulescu, , „Glass-ceramic foams made of very high coal fly ash weight ratio by the direct microwave heating technique", Journal La Multiapp, vol. 1, no. 4, 2020, pp. 33-42. https://doi.org/10.37899/journallamultiapp.v1i4.242

[11] L. Zeng, H. Sun, T. Peng, „Effect of borax on sintering kinetics, microstructure and mechanical properties of porous glass-ceramics from coal fly ash by direct overfiring", Frontiers in Chemistry, Inorganic Chemistry Section, 2022. https://doi.org/10.3389/fchem.2022.839680

[12] Y. Dong, J-E. Zhou, B. Lin, Y. Wang, „Reaction-sintered porous mineral-based mullite ceramic membrane supports made from recycled materials", Journal of Hazardous Materials, vol. 172, no. 1, 2009, pp. 180-186. https://doi.org/10.1016/j.jhazmat.2009.06.148

[13] C. Bray, „Dictionary of glass. Materials and techniques", 2nd edition, A & C Black, London and Pennsylvania Press Philadelphia, 2001. http://book.google.ro

[14] ***„Borax-Anhydrous and hydrated", Technical Bulletin, Klen International Pty. Ltd., Chatswood, New South, Australia, 2016. https://environex.net.au/wp-content/uploads/2016/04/Borax-Anhydrous-and-hydrated.pdf

[15] G. Scarinci, Giovanna Brusatin, E. Bernardo, „Glass Foams" in Cellular Ceramics: Structure, Manufacturing, Properties and Applications, Wiley-VCH Verlag GmbH & Co KGaA, M. Scheffler, P. Colombo eds., Weinheim, Germany, 2005, pp. 158-176.

[16] Vilma Ducman, „Foaming process of waste glass using $CaCO_3$, MnO_2 and water glass as foaming agent", International Conference Sustainable Waste Management and Recycling. Glass waste, pp. 59-66, Kingston University of London, UK, 2004.

[17] K.S.P. Karunadasa, C.H. Manoratne, H.M.T.G.A. Pitawala, R.M.G. Rajapakse, „Thermal decomposition of calcium carbonate (calcite polymorph) as examined by in-situ high-

temperature X-ray powder diffraction", Journal of Physics and Chemistry of Solids, vol. 134, 2019.

[18] D.A. Jones, T.P. Lelyveld, S.D. Mavrofidis, S.W. Kingman, N.J. Miles, N.J., „Microwave heating applications in environmental engineering–A review", Resources, Conservation and Recycling, vol. 34, no. 2, 2002, pp. 75-90.

[19] Helen J. Kitchen, S.R. Vallance, Jennifer L. Kennedy, Nuria Tapia-Ruiz, Lucia Carassiti, „Modern microwave methods in solid-state inorganic materials chemistry: From fundamentals to manufacturing", Chemical Reviews, vol. 114, no. 2, 2014, pp. 1170-1206.

[20]*** „Metrology in laboratory-Measurement of mass and derived values", Radwag Balances and Scales, 2nd edition, Radom, Poland, 2015, pp. 72-73. http://www.radwag.com

[21] L.M. Anovitz, D.R. Cole, „Characterization and analysis of porosity and pore structures", Reviews in Mineralogy and Geochemistry, vol. 80, 2005, pp. 61-164.

[22] R.D. Rawlings, J.P. Wu, A.R. Boccaccini, „Glass-ceramics: Their production from wastes-A review", Journal of Materials Science, vol. 41, 2006, pp. 733-761.

[23] L. Paunescu, M.F. Dragoescu, S.M. Axinte, „Thermal insulating material with high mechanical strength made from clay brick waste and coal ash using the microwave energy", Journal of Engineering Studies and Research, vol. 26, no. 2, 2020, pp. 28-34.

Advanced electric drives in the wind turbine conversion chain

Actionarile electrice avansate in lantul de conversie al turbinelor eoliene

Emilia Dobrin[1]

[1]Timișoara Polytechnic University
Victoriei Square 2, Timișoara 300006, Romania
E-mail: emi_dobrin@yahoo.com

Rezumat: *Creşterea consumului de energie şi al emisiilor de gaze cu efect de seră (GES) are consecinţe din ce în ce mai grave asupra mediului, societăţii şi economiei, atât la nivel global, european, cât şi naţional. În acest context lupta pentru măsuri de combatere a efectelor schimbărilor climatice impune stabilirea de strategii energetice şi ecologice. La nivel european s-a stabilit neutralizarea emisiilor de gaze cu efect de seră până în 2050, îmbunătăţirea eficienţei energetice şi promovarea surselor regenerabile de energie. Utilizarea resurselor eoliene, în special a turbinelor eoliene cu generatoare sincrone cu magneţi permanenţi şi a diverselor actuatoare electrice avansate - convertoare de mare putere, se accentueaza tot mai mult.*
Această lucrare este un studiu bibliografic elaborat al compoziţiei, tehnologiilor şi configuraţiilor de ultimă generaţie a lanţului de energie eoliană a unui parc eolian. Sunt abordate şi studiate tendinţele actuale ale diferitelor topologii din lanţul de conversie a energiei eoliene disponibile în literatură.

Cuvinte cheie: actuatoare electrice avansate, conversie de energie, configuraţie electrică.

Abstract: *The increase in energy consumption and emissions of greenhouse gases (GHG) has increasingly serious consequences on the environment, society and the economy, both at the global, European and national level. In this context, the fight for measures to combat the effects of climate change require the establishment of energy and ecological strategies. At the European level, the neutralization of greenhouse gas emissions by 2050, the improvement of energy efficiency and promotion of renewable energy sources have been established. The use of wind resources, especially wind turbines with permanent magnets synchronous generators and various advanced electrical actuators - high power converters, is increasingly emphasized.*
This paper is an elaborate bibliographic study of the state-of-the-art wind power chain composition, technologies and configurations of a wind farm. The current trends of the different topologies in the wind power conversion chain available in the literature are addressed and studied.

Keywords: advanced electric actuators, energy conversion, electrical configuration.

1. Introduction:

The development of power electronics and control electronics led to the emergence of an informational flow that complemented the existing electrical drive systems, bringing them to the level of advanced electrical drives [1].

The main purpose of an electric drive is to drive, electrically, working machines, mechanical devices, in our case to an electric generator. Another role of an actuation is that of matching the motor/electric generator to the mechanical load and to the electrical network [2, 3].

Advanced Electric Actuators (AEAs) power electronic devices to (digitally) control this power conversion process [4].

The electric drive system (SAE) will therefore represent the set of devices that transform electrical energy into mechanical energy and control this energy.

Electric drives have the largest share in electricity consumption. It is stated that over 60% of the electricity produced is used in electric drives [1].

The advantages of using AE in various industries: reliability, precision, speed, improving the quality of dynamic processes, reducing consumption by 30-50%, compatibility of AE with power and information systems, fine adjustments, starting, stopping and reversing the direction of rotation, high efficiency, easy maintenance [5].

Among the most important fields of use of AEA would be: - renewable energies, the technological industry, the automotive industry, the military industry, the aeronautical industry, the cement industry, the metallurgical industry, electrified transport, info gadgets, home applications, etc. [3, 6].

The importance of AEA in the field of renewable energies is maximum. Today's turbines, represented in figure 1, are able to transform a large amount of wind energy into electricity. This is due to blades that are developed using cutting-edge aerodynamic analysis and performance-enhancing electronics.
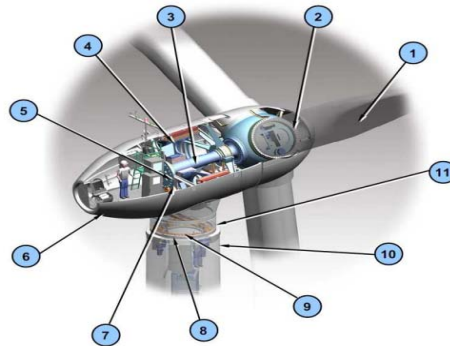
Fig.1 Representation of the main components of a wind power plant:1-blade, 2-blade system orientation, 3-main transmission system, 4-electric generator, 5- bracking rotor system, 6-nacelle, 7- bracking system, 8-rotor system orientation, 9-braking system of the braking device [7]

The main elements of a wind energy conversion system are shown in figure 2: the turbine rotor with the component blades, and the gearbox, which may be missing in the case of using synchronous generators, participates in the conversion of wind energy into mechanical power. The electric generator, which can be synchronous or asynchronous

(induction), transforms mechanical energy into electrical energy that will be processed with the help of high-power converters to be transmitted to a step-up transformer from where it is taken over by the network [8].

2. Advanced electric drives. Topologists, classifications

The advanced electric drives are composed of the following parts, described in figure 2.1: electric generator, electronic power converter, current and position sensors, unit controller.
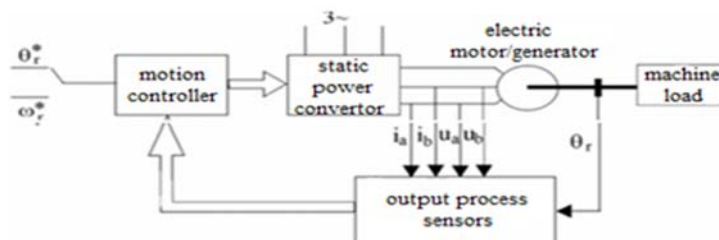
Fig. 2.1. The basic topology of an advanced electric drive [5].

The drive controller can also be motion – speed and/or position controller, more or less the same for all types of electric drives and the electric controller that deals with current and voltage (or link flux and torque) control within a converter [3].
Electrical sensors (observers) refer to voltage, current, flow measured (or calculated) state variables while motion sensors (observers) mean position and/or speed and torque according to measured (or calculated) state variables [3].
The electrical controller generally has electrical input sensing (observer) from both the power supply and the PEC output. The motion controller generally only handles motion sensor (observer) outputs. On the other hand, electrical controller commands are related to power source-side energy conversion performance commands (unity power factor, harmonic elimination) while motion controller commands are related to motion control commands (speed, position, torque) managed through an interface from a local digital controller. As expected, the electrical and motion controllers are mixed together in the hard and soft drive controller. So far both the drive controller and the interface are made by high-performance digital signal processors (DiP). Electric controllers tend to be more specific and have applications for different electric drives [3].
High power converter
It is a regulation system that transforms the single-phase supply voltage into a three-phase voltage system where the voltage and frequency are variable, obtained by pulse width modulation (PWM), as shown in figure 2.2. The adjustment of the parameters specific to the static converter are set by means of a galvanically isolated serial communication (SCI).
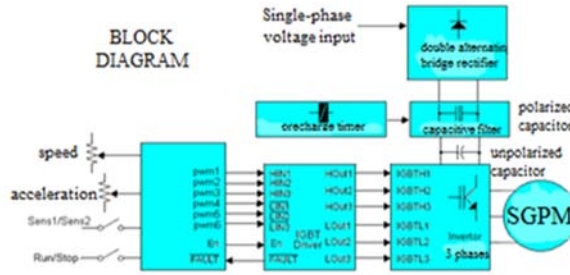
Fig. 2.2. Block diagram representation of the static converter [9]

3. Topologies of the advanced electric drives of wind power plants

The configuration of the wind power plants includes a multitude of constructive variants with advanced electric actuators, which will be presented below.

Depending on the type of connection of the electrical generators to the electrical network we have:

- direct: cheap, but with low energy yield, as can be seen in figure 3.1a;

- indirectly: more expensive as a result of the cost of static equipment, but with higher efficiency because driving strategies can be realized that tend to operate at the points of maximum power, at variable wind speeds figure 3.1b, presented in [10].

Direct connection implies rigid connection to the alternating current (usually three-phase) of the network. The indirect connection to the network involves passing the current from the generator through a series of electronic devices that have the role of adjusting the current to match that of the network. In the case of asynchronous generators, this is achieved by simply connecting to the network [10].

a)   b)
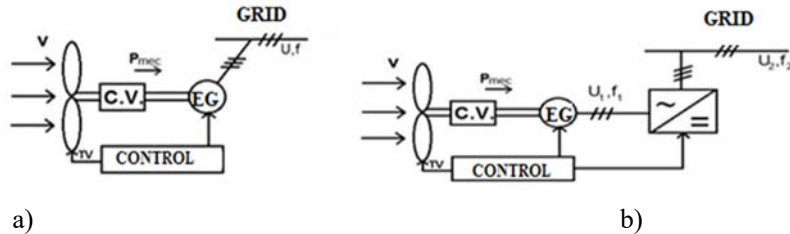
Fig. 3.1. The type of connection of the SGPM to the grid: a) direct connection; b) indirect connection [10].

Currently, the wind control systems that operate at wind speeds that vary significantly over time are built in the second variant, and those that operate at an approximately constant wind speed, in the first variant. In the absence of the fixed voltage and frequency network, the energy provided by the electric generator can be stored in the electric accumulators (AE), from figure 3.2:
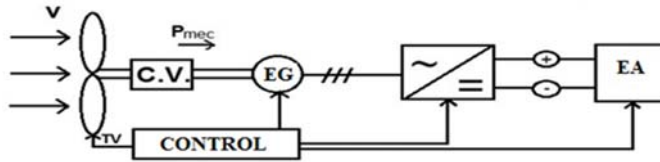
Fig 3.2. Wind system charging on electric accumulators [10]

In the absence of wind, the energy needed by the consumers is given from the AE. In this case, power fluctuations do not create problems for electric consumers, because the voltage at AE is approximately constant.

In this classic topology representing the conversion of wind energy into electrical energy, the turbine shaft can be directly connected to the gearbox or the generator. The generator with permanent magnets is chosen because the sliding contacts are eliminated, which leads to the reduction of the size of the generator, simplifies their maintenance, low price. The connection diagram is shown in figure 3.1 below [11].
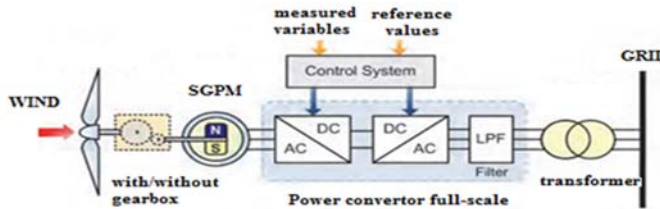
Fig. 3.1 Common model of energy conversion of a wind power plant [11]

The SGPM is connected with a high-power converter, the generator can completely disconnect from the grid and operate at full speed. In the full converter concept, the converter ensures the decoupling of the generator and the mechanical transmission from the mains. This type of converter being efficient and complex, but has a high price which makes the price of the whole conversion system quite high. The electrical energy that is produced is passed through cables to the base, where a step-up transformer is placed [11, 13]. All the generated power goes through the converter to the grid.

In this constructive options in figure 3.2, the high-power converter is connected to the SGPM and provides protection against faults occurring in the wind turbine network. In SGPM the frequency varies according to the wind speed, which allows the wind turbine to operate at variable wind speeds being a great advantage for the system, therefore a Chopper converter is required [14].
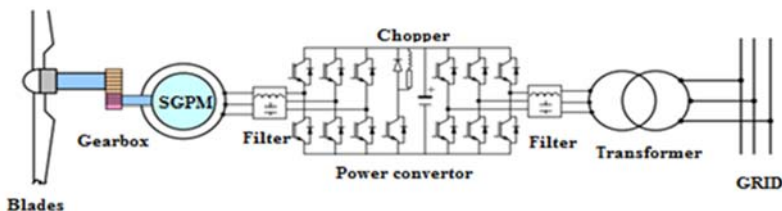
Fig. 3.2. Topology of a wind power plant conversion chain [14]

In order to efficiently control the electric generator but also the flow of active and reactive power to the network, a Chopper type converter is chosen. The rotor-side converter ensures the regulation of the rotation speed in a wide range, while its grid-side converter transfers the active power to the grid and tries to cancel the reactive power consumption.

A great advantage of this topology is that it allows the integration of considerable capacities in the network.

The disadvantage of this switching strategy is the double switching losses, as the two power transistors are switched simultaneously (instead of one at a time) [14].

The configuration in figure 3.3 is suitable if one wants to use the maximum power point tracking (MPPT) control strategy based on the perturbation and observation (PO) method in low power wind turbines by maximizing the output power. It presents the advantage of increasing the output power by more than 50% improving the performance of wind systems, by eliminating the oscillation problems that occur due to power fluctuations when it reaches the maximum value [15].
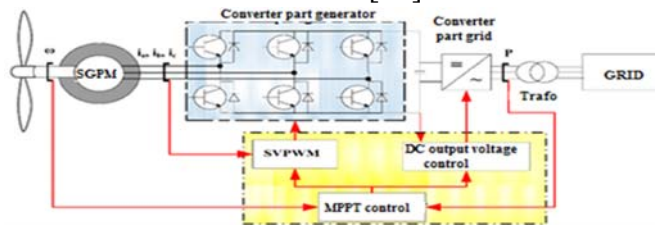
Fig. 3.3 Electricity conversion scheme [15]

The system comprises a wind turbine, SGPM, a rectifier, MPPT and an inverter. The turbine transforms the wind into mechanical energy, the SGPM transforms the mechanical energy into electrical energy, and the rectifier ensures the transformation of the electrical voltage from a.c. in d.c. This is due to the fact that the speed of the rotor increases with the increase in wind speed, which also affects the power generated.

In addition, MPPT maximizes the output power of the wind turbine system and the inverter converts direct current into alternating voltage. Applying this scheme to the wind system, especially at high wind speeds, has significant results in increasing SGPM voltage and power [15].

In figure 3.4, a high-speed static converter participates in the wind-electric energy conversion.

In figure 3.4, a high-speed static converter participates in the wind-electric energy conversion.
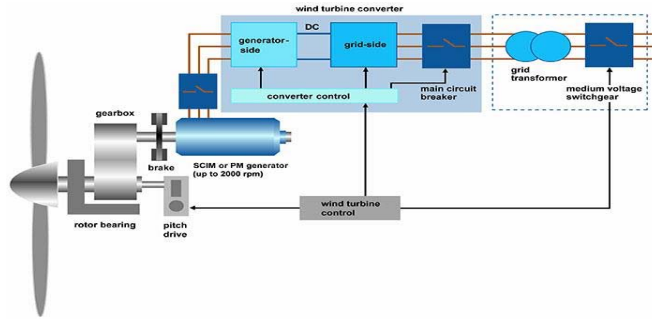
Fig. 3.4 The wind conversion chain having a high speed converter [16].

HSFC High Speed Converter - provides SGPM speed and torque control. This type of converter presents the advantages: small size of the SGPM, small volume of the converter.

Using a SGPM in a wind system results in high power density and small dimensions with the highest efficiency at all speeds, providing the maximum annual energy production at the lowest lifetime cost [16].

The two-level converter is an ac-dc-ac converter, with six unidirectionally driven insulated gate bipolar transistors (IGBTs) used as the rectifier and the same number of unidirectionally driven IGBTs used as the inverter.

In this energy conversion of the wind system, the rectifier is connected between the SGPM and the capacitor bank as seen in figure 3.4. The inverter is connected between this bank of capacitors and a second-order filter, which in turn is connected to the power grid [17, 18].
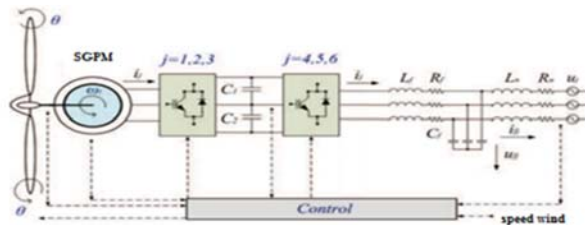
Fig. 3.4 Turbine conversion using a multilevel converter with capacitors [18]

With this configuration, it is desired to obtain a sinusoidal voltage through several voltage levels having voltages with capacitors as a source. They are used for wind power plants of medium or high power.

Among the advantages are the reduction of switching losses of the converter by up to 25% compared to the simple one, the efficiency of the converter is greatly improved.

A disadvantage of this type of capacitor is the voltage imbalance between the top and bottom capacitors, but also unequal stress on the semiconductor devices.

 The matrix converter is an ac-to-ac converter with nine isolation bi-directionally driven bipolar gate transistors (IGBTs). The matrix converter is connected between a first order filter and a second order filter. The first-order filter is connected to a SGPM, while the second-order filter is connected to the mains. The configuration of the

simulated wind energy conversion system with the matrix converter is presented in figure 3.5 [18].
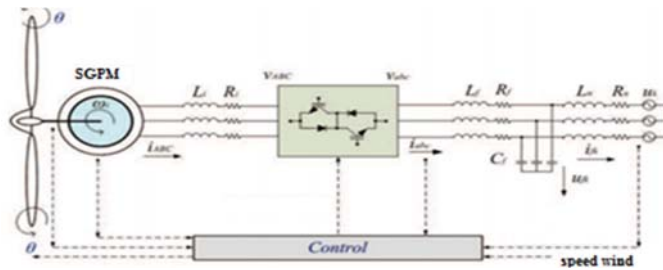
Fig. 3.5. Turbine conversion using a matrix converter [18]

This conversion has the advantages:
- compared to classic converters, they have reduced dimensions and dimensions, due to the absence of DC-link capacitors;
- the absence of the DC-link capacitor increases the efficiency and lifetime of the converter;
- the switching losses of the matrix inverter are reduced compared to the back-to-back one;
- the sinusoidal waveforms of the input and output currents show negligible harmonics;
- the thermal stresses are reduced compared to the classic converter.
 Disadvantages of this energy conversion:
- the maximum output voltage of the matrix converter is 0.866 times higher than the input voltage;
- due to the absence of the DC link, there is no decoupling between the input and output of the converter;
- the modulation technique and switching control are more complicated than those of conventional inverter PWM;
- the protection of the matrix converter in fault situations is weak.
For applications of medium or high power wind power plants, three types of multilevel converters can be used: fixed Neutral Point (CPN), Fly capacitor (CF), series converters with H bridge (CSPH).
The CPN multilevel converter shown in figure 3.6 is a power converter that can operate in inverter or rectifier mode [19].
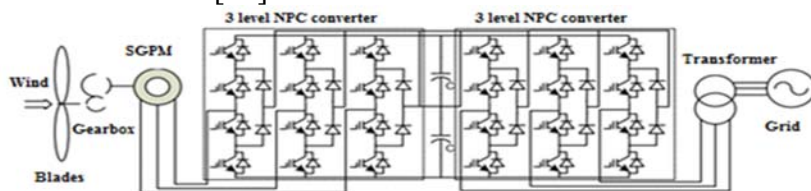
Fig. 3.6 Wind power generation system based on multilevel converter fixed at neutral point [19]

At the CPN converter the d.c. voltage of the bus is divided into voltage levels by series capacitors, the neutral point is connected to the midpoint of the DC connection, which allows this topology to form back-to-back connections. CPN is a three-level back-to-back converter.

Through this energy conversion, the CPN converter is intended to improve its operation in stationary and transient conditions. When n is large enough, the number of diodes required will make the system impossible to implement; the number of diodes required for each phase will be (2n-4). Therefore, this topology is not suitable for high power applications.

CPN has advantages:
- the CPN converter has the capacity to handle high voltage;
- reduced switching losses;
- high efficiency compared to other types of converters;
- reduces the filter elements, which affect the dynamic response of the converter.
 Limitations of CPN converters:
- requires semiconductor devices;
- between the upper and lower DC-link capacitor the voltage is unbalanced [19].

This wind-energy conversion shown in figure 3.7 is composed of a voltage Z converter or Z source converter, and is the power converter supplied with "impedance". It is mainly used for power conversions d.c.-d.c., a.c.-d.c., a.c.-a.c. and d.c.-a.c. This converter offers a new type of power conversion, compared to the classic one.
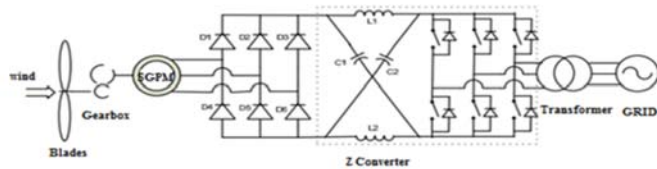
Fig.3.7 Energy conversion configuration with a Z-converter [19]

Inductors L1 and L2 and capacitors C1 and C2 are linked in an X-shape, being used to provide an impedance source that connects the converter to the DC source, load or other converter.

In order to increase the performance of a wind conversion system, the behavior of the Z converter in stationary and transient mode is analyzed, especially due to its low cost and high efficiency. It also has other advantages: fewer components than the classic converter, smaller dimensions, the output voltage differs from the input voltage.

Disadvantages: it requires high voltage Z capacitors which increases the cost of the converter as well as its size, it can cause overvoltages which leads to the destruction of the device, it is a unidirectional converter [19].

In this variant, the fuzzy logic controller shown in figure 3.8 is usually used to adjust the pitch angle of the blade. This technique is based on human experience using a set of rules determined by applying linguistic variables instead of numerical ones [20].
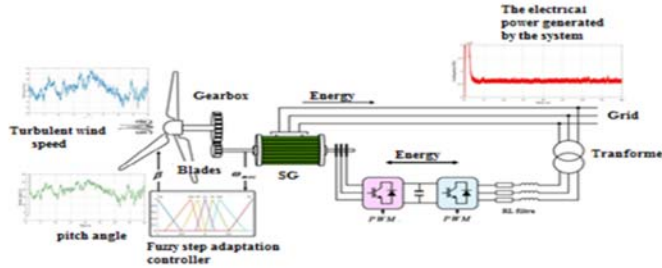
Fig. 3.8 Wind conversion system with Fuzzy controller [20]

The fuzzy logic process has three main phases: fuzzification, inference, defuzzification.

Making comparisons between three types of CLF configurations: CLF with initial parameters, optimized CLF, adaptive CLF and two classic control methods: the classic PI controller and the programmed PI controller, it was found that the Fuzzy optimized CLF and the PI controller have the same results, being able to replace one controller with the other.

Advantages: improves the quality of power produced by the wind system, achieves precise regulation of generator speed and electrical power and mitigates the effects of mechanical loads compared to other controllers, as well as the ability to produce more energy annually.

4. Conclusions:

Some representative examples from the existing configurations for modern wind power plants were selected from the specialized literature.

Internationally, there is a growing trend of using permanent magnet synchronous generators in wind power plant applications due to the significant advantages: sliding contacts are eliminated, which leads to a reduction in the size of the generator, simplifies their maintenance, low price, but above all because it works at variable wind speeds.

The quality of the electricity supplied in the power grid is influenced by the location of the wind power plant and the choice of the common point of connection to the grid. The closer the wind power plant is located to the consumers, the higher the quality of the electricity supplied to the network.

The wind conversion system that has the electronic part provided by a full-scale converter, being a complex converter, provides SGPM with the possibility to completely disconnect from the grid to operate at maximum speed although its cost is high. If we opt for an HSFC converter we will have SGPM speed and torque control, being a low volume converter which helps to reduce the footprint and SGPM and to the whole wind system it offers the maximization of energy production at a reduced price over the lifetime of the converter.

If you choose to use a chopper-type power converter in the energy conversion, the losses are doubled due to the two transistors in its composition that switch simultaneously.

Control strategies are used to increase the performance of the wind system. The MPPT control method is often used in conjunction with other control methods. When used with the PO (perturb and observe) method, over 50% improvement in system performance is found as well as raising the output voltage and power at the SGPM. If the TSR+MPPT method is chosen, a higher quality of the output voltage and a fast response time are obtained.

The latest generation converters include the multilevel, matrix, multilevel CPN, or Z type used in applications for medium to high power wind power plants, which improve the efficiency of the entire wind system. Due to their characteristics, switching losses are reduced, they have reduced geometric dimensions compared to classic ones, the lifetime of the converter is increased, the number of filter elements is also reduced, they can have high prices compared to classic capacitors.

If one opts for the wind turbine variant equipped with a fuzzy logic controller, the SGPM speed will result in a higher quality power, the speed and electrical power of the SGPM being regulated quite precisely, and the annual energy production is high.

There are a multitude of combinations for wind energy conversion, from which one essential thing emerges, namely that there is no universally valid variant that is satisfactory from all points of view.

Bibliography

[1]*** em.uvc.ro – Curs AE, Mihai Linca, 2018;
[2] W. De Doncker, A. Veltman, Advanced Electrical Drives: Analysis, Modeling, Control, ed. Springer, 2011;
[3] ***ACADEMIA – Sisteme de acționare electrică, curs;
[4] ***REGIELIVE – Acționări electrice, curs;
[5] I. Boldea, S. Nasar, Electric Drives, ed. CRC Press, 2017;
[6]***PDFFACTORY - Elemente generale ale sistemelor de acționare electrică, curs;
[7]***ARPMGL - Raport privind Impactul asupra Mediului Centrală electrică eoliană Pechea;
[8] J. Manwell, J. McGowan, Wind Energy Explained: Theory, Design, and Application, 2nd ed. Hoboken, NJ, USA: Wiley, 2009, ISBN: 978-0-470-01500-1;
[9] ***www.emil.matei.ro/csf.php;
[10] I. Popescu, Studii și cercetări privind optimizarea sistemelor eoliene, teză de doctorat, Politehnica, 2017;
[11] H. Duc, H. Le Thai, A Study of Optimizing a Wind Power Station in an Isolated Region Based on Specifications, 12th IEEE Conference on Industrial Electronics and Applications (ICIEA), 2017, pg.483-489;
[12] M. G. Molina, J. M. G. Alvarez, Technical and Regulatory Exigencies for Grid Connection of Wind Generation, Smart Grids: Hybrid Microgrids (AC/DC) Implementation, Wind Farm – Technical Regulations, Potential Estimation and Siting Assessment, ISBN 978-953-307-483-2, pg. 1-29;
[13] V. Yaramasu, B. Wu, M. Rivera,''A new power conversion system for megawatt PMSG wind turbines using four-level converters and a simple control scheme based on two-step model predictive

strategy Part I: Modeling and theoretical analysis'' IEEE J. Emerg. Sel.Topics Power Electron, vol. 2, no. 1, ISSN 2168-6785, 2014, pp. 3–13;

[14] S. Kabashia , G. Kabashi, Modelling, Simulation and Analysis of Full Power Converter Wind Turbine with Permanent Synchronous Generator, Chemical engineering transactions vol. 34, 2013, ISBN 978-88-95608-25-9;

[15] R. Syahputra, I. Soesanti, Performance Improvement for Small-Scale Wind Turbine System Based on Maximum Power Point Tracking Control, Energies 12(20), Section A: Electrical Engineering, 2019, 3938, pp. 1-18;

[16] ***ABB – High speed full converter, concepts;

[17] B. Shanmugan, R. Deekshit, C.R Prahallad, "Design and implementation of power electronic converter in wind turbine system," International Conference on Smart grids, Power and Advanced Control Engineering (ICSPACE), 2017, pp.106 – 113;

[18] R. Melício, F. Mendes, Wind Turbines with Permanent Magnet Synchronous Generator and Full-Power Converters: Modelling, Control and Simulation, Portugalia, ed. Interchopen, (2015), ISBN978-953-307-221-0, pp.465-495;

[19] Md R. Islam, Y. Guo, Power converters for wind turbines: Current and future development, Materials and processes for energy: communicating current research and technological developments, Energy Book Series-2013, Formatex Research Centre, (2013), p.559–571;

[20] O. Zamzoum, A. Derouich, Performance analysis of a robust adaptive fuzzy logic controller for wind turbine power limitation, Journal of Cleaner Production, Elsevier Ltd, (2020), S0959-6526(20)31706-6.

Running a hydronic balancing simulator in Microsoft Excel

Rularea unui simulator de echilibrare hidrică în Microsoft Excel

Ciprian Bacoţiu[1], Peter Kapalo[2], Constantin Cilibiu[1]

[1] Technical University of Cluj-Napoca, Romania
Building Services Engineering Faculty, Department of Building Services Engineering
B-dul 21 Decembrie 1989, nr. 128-130, Cluj Napoca, România
g/o ckʁ'ekr tkcpQlceqvkvB kpvɪc0wenvl0q."eqpɪvcpvkpQekkdkvB kpvɪc0wenvl0q"

[2] Technical University of Košice
Civil Engineering Faculty, Institute of Building and Environmental Engineering
Vysokoskolska 4, 04200, Košice, Slovakia
g/o ckʁ'r gvgt0ncr cnqB wngQun6

Abstract. *Providing the required indoor comfort at minimal operating costs is the main objective of every HVAC system. However, despite the fact that in theory, each design effort promises to deliver the design flow at each heating or cooling unit, in reality this is not happening too often. The role of balancing is to obtain the design flow at each terminal unit, by installing some specialized valves and applying a coherent procedure of setting and adjustment. This paper presents a simple hydronic balancing simulator, implemented in a Microsoft Excel spreadsheet. The model uses static STAD balancing valves, provided by the Swedish manufacturer Tour Andersson. The main purpose of the simulator is to obtain a learning tool for students or young engineers, allowing them to observe and understand the circuits interactions when running balancing procedures.*

Key words: hydronic balancing, simulator, Excel, balancing valves, Tour Andersson

1. Introduction

Providing the required indoor comfort at minimal operating costs is the main objective of every HVAC system. However, despite the fact that in theory, each design effort promises to deliver the design flow at each heating or cooling unit, in reality this is not happening too often. If no balancing measures are taken, the circuits situated closer to the pump will be usually favoured, by having overflows, at the expense of other circuits that will experience underflows. The purpose of balancing is to obtain the design flow at each terminal unit, by installing some specialized valves and applying a coherent procedure of setting and adjustment: while these balancing valves are chosen and preset at design time, an on-site adjustment is always necessary.

Therefore, the balancing procedure is extremely important and needs to be carefully carried out.

This paper presents a simple hydronic balancing simulator, implemented in a Microsoft Excel spreadsheet. The model uses static STAD balancing valves, provided by the Swedish manufacturer Tour Andersson. This choice was natural, since our Hydraulics Laboratory is fitted with such valves and we use them for many years.

The idea of making software hydronic simulators is not new. Usually, balancing valve producers have such tools for training and design purposes. But these proprietary software is either not freely available or it is limited to the producers' specific valves ([1], [2]). Therefore, our goal was to create an in-house simple simulator that would become a valuable learning tool for students or young engineers, allowing them to observe and understand the circuits interactions when running balancing procedures.

2. Basic hydronic balancing theory

According to [3], one balancing valve positioned near each terminal unit is sufficient to create the correct distribution of flows in the system. But when the flow is adjusted in one valve, pressure drops also change in pipes, valves and accessories, thus modifying the differential pressure across other balancing valves. These interactions among circuits are unavoidable, therefore without having a coherent balancing procedure, there is a danger to never obtain the required flows, even after a long series of tedious and repeated maneuvers and corrections. To avoid this danger, it is required to divide the plant into modules. A module contains several terminal units connected in parallel (each having its own balancing valve), controlled by a common balancing valve (Figure 1).
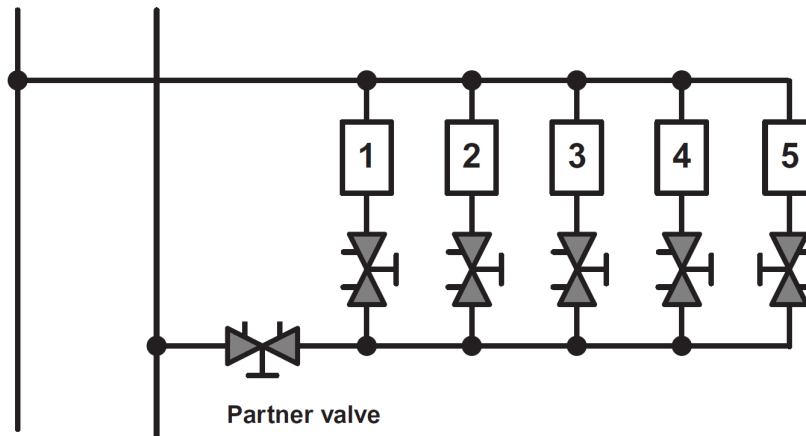
Fig. 1. A module example with conventional valve naming [3]

This common valve is named partner valve and its role is to balance all units of a module against each other, by compensating the disturbances created by each flow adjustment [3]. This is possible because the so-called law of proportionality applies: an external disturbance affects the flows in all terminal units in the same proportion.

Therefore, adjustments will start from the circuit furthest away from the partner valve (called reference valve, e.g. valve no. 5 in Figure 1). Then terminal 4 will be

adjusted, disturbing terminal 5, until 4 and 5 are balanced with each other in the same flow ratio (usually >1). Thus, 4 and 5 will respond in the same proportion when an external disturbance to them will arise. So, when terminal 3 will be adjusted, it will disturb 4 and 5 to the same extent, yet that adjustment must allow a common flow ratio for all the valves 3, 4 and 5. It means that these valves are balanced with each other. The procedure continues until the entire module is balanced at a certain flow ratio. In the end, the overflow will be compensated (for the entire module) from the partner valve.

3. Using Microsoft Excel as a framework for the hydronic simulator

In order to simulate the previously described procedure, we needed to choose some balancing valves for the model and a software framework to implement the equations. The choice for the balancing valves was rather easy, as we worked for many years in our Hydraulics Laboratory with static STAD valves, provided by the Swedish manufacturer Tour Andersson. These STAD valves are characterized by the Kv factor/coefficient, which increases with the valve opening (Table 1).

Table 1

Kv values for PN-25 STAD valves [4]

Turns	DN 10	DN 15	DN 20	DN 25	DN 32	DN 40	DN 50
0.5	-	0.136	0.533	0.599	1.19	1.89	2.62
1	0.091	0.226	0.781	1.03	2.09	3.40	4.10
1.5	0.134	0.347	1.22	2.13	3.36	4.74	6.76
2	0.264	0.618	1.95	3.64	5.22	6.25	11.4
2.5	0.461	0.931	2.71	5.26	7.77	9.16	15.8
3	0.799	1.46	3.71	6.65	9.82	12.8	21.5
3.5	1.22	2.07	4.51	7.79	11.9	16.2	27.0
4	1.36	2.56	5.39	8.59	14.2	19.3	32.3

The Kv factor depends on the differential pressure and flow, as shown in Eq. 1:

$$Kv = 0.01 \frac{q}{\sqrt{\Delta p}} \quad [\text{-}] \quad (1)$$

where:
Kv   - flow factor [-],
Q   - flow [l/h],
Δp   - differential pressure [kPa]

The software framework chosen for implementing the simulator was an Excel spreadsheet, because it offers both an easy graphical interface and a nice programming environment for writing the equations.

The prototype of the simulator had to be simple. At this stage it has only one module with four terminal units (Figure 2). In order to simplify the graphical interface, only the return pipes were represented, because traditionally the STAD valves are placed there. Each terminal unit is characterized by a design flow and a pressure drop

(yellow cells). Pump parameters are known and also pressure drops on the riser are known (yellow cells). For simplicity, we assumed that horizontal pipes have negligible head losses. Each STAD is clearly visible as a small image, accompanied by a SpinButton showing its setting (with a precision of one hundredth of a turn). Underneath each valve, its differential pressure is shown (Figure 2). Also, each STAD can be quickly shut off using a CheckButton, allowing us to simulate a zero-flow situation.
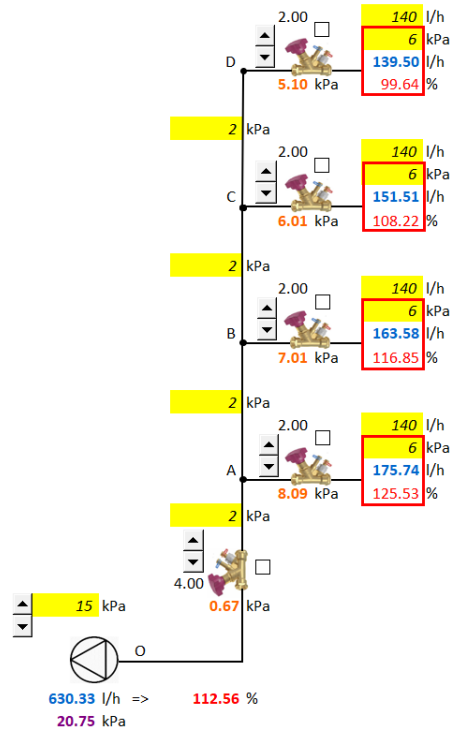
Fig. 2. The hydronic simulator interface during an exercice

The valve opening had to be related to its Kv, therefore a function Kv=f(turns) was implemented for each STAD valve of the module. This function was written in the VBA programming language (Visual Basic for Applications), using a linear interpolation algorithm based on the values from Table 1. For simplicity, only DN 15 STAD valves were used.

Then, classical hydraulics equations were written (such as flow conservation in each node and Bernoulli's equation) following a special approach given by [5] and taking into account each series and parallel configuration. It should be noted that the novelty of this approach consists of thinking that every element of the module has a Kv, not only the valves, but also the pipes and the terminal units.

As *modus operandi*, the simulator is mouse-driven: by (left) clicking on the SpinButton of a balancing valve, the number of turns is modified, this changes Kv, then the flow and differential pressure are modified, with influence on all other circuits...

This dynamic interactivity is the major advantage of the simulator. In real-life hydronic circuits, several expensive measurement tools (e.g. TA Scope) would be necessary to observe and understand the phenomenon.

4. Working with the hydronic simulator – applying the proportional method

In a specific dataset configuration used as an exercise, the aim of running the simulator is to obtain the design flow on each terminal unit, by adjusting each balancing valve opening position with the mouse. The recommended precision for obtaining the flows by Tour Andersson is ±10%.

In this example, we started with all the balancing valves with a presetting of 2 turns (Figure 2), i.e. the middle opening, and we applied the proportional method for balancing the module. This presetting of 2 turns may also be considered as a rule of thumb for all the valves of a module in order to ensure enough differential pressure (3kPa for the TA Scope instrument in real-life measurements). Anyway, our simulator makes the calculations even if the pressure drop in the balancing valves is under that threshold of 3 kPa. But if we want to simulate exactly the real-world measuring device and also to optimize our module, we need to impose 3 kPa at design flow on the most unfavoured circuit and find the corresponding valve setting.

But let's assume first that we are not interested in any optimization. The target of the exercice is to obtain 140 l/h in each terminal unit. The partner valve is fully open (4 turns).

The most unfavoured circuit is no. 4, because it gives the smallest flow ratio - lambda (99.64%). So we adjust the balancing valve no. 3 until its flow ratio is the same as for the valve no. 4. The common flow ratio will be very close to 101%. This gives a setting of 1.83 for the valve no. 3. Now, these two valves are balanced to one another and will react in the same proportion to external disturbances. Then, valve no. 2 will be adjusted in order to obtain the same flow ratio as valves no. 3 and 4. The common flow ratio for these three valves will be very close to 102.5%. This gives a setting of 1.71 for the valve no. 2. Finally, valve no. 1 will be adjusted in order to obtain the same flow ratio as the other three valves. The common flow ratio for all four valves will be very close to 104.3%. This gives a setting of 1.63 for the valve no. 1. In the end, in order to obtain the design flow for each valve (i.e. to bring the flow ratio close to 1), the overflow will be taken away from the module by closing the partner valve to a new position, 2.74 (Figure 3a).

The balancing procedure succeeded to obtain the desired flows, but the solution is not optimized, because the index valve (no. 4) has too much differential pressure (anything above 3 kPa is considered a waste of energy).

In the next stage, we can try to optimize the solution, by imposing 140 l/h and 3 kPa on the valve situated on the most unfavoured circuit, i.e. the circuit no. 4. The setting of the valve no. 4 is determined by using some Tour Andersson specialized software (HyTools or HySelect) or a nomograph. Since HyTools is freely available on the Android platform and it is very easy to use on a smartphone, we definitely

recommend it. So, from HyTools we found that the setting for the valve no. 4 must be 2.33 (instead of 2.00 - the initial guessed/customary non-optimized presetting).

Repeating the whole proportional procedure again for the rest of the valves, we obtained the optimized solution for the entire module, all flows being very close to 140 l/h and the index valve having a differential pressure of about 3 kPa. Not exactly 3kPa, but close enough, due to precision issues generated by the linear interpolation assumption.

If we compare the two solutions, it can be noticed that for the optimized method, each balancing valve is more opened (having less pressure losses), while the partner valve is more closed than in the non-optimized method (Figure 3b).

For the optimized solution, the partner valve is closed to 2.37 turns and its differential pressure, 4.84 kPa, actually reveals the excess pressure at the pump. Thus, the pumping costs can be minimized, i.e. the pump can operate at a lower head [3].
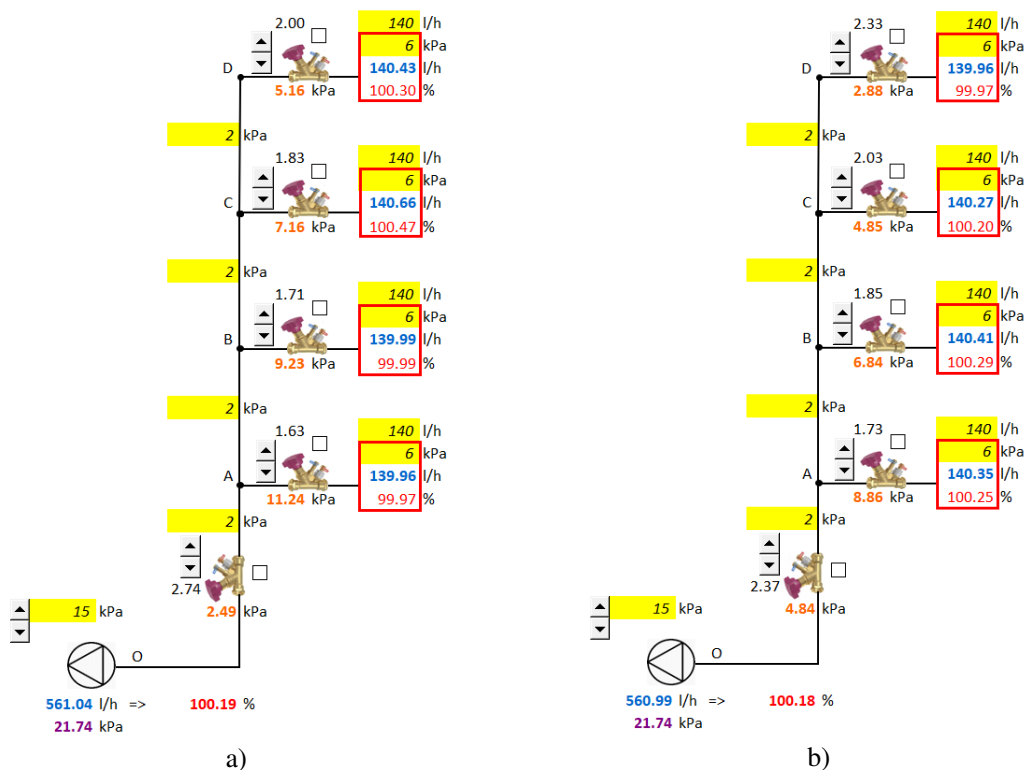
Fig. 3. The module is finally balanced: a) non-optimally b) optimally

5. Conclusions

For the moment, our hydronic simulator has only one module with four circuits, but it gives the expected results and fulfills its purpose. We are using it as a learning tool for students and young engineers, in their quest to observe and understand the circuits interactions when running balancing procedures. It is a project under development and it will be certainly improved in the future: we expect to have 4

connected modules with a total number of 16 terminal units, using different types of valves, different terminal units with different design flows and different pressure losses.

References

[1] *** Hydronics Design Studio, https://www.hydronicpros.com/downloads/index.php?id=21, accessed October 2022

[2] *** Belimo Hydronic Simulator, https://www.belimo.com/us/en_US/support-am/sizing-and-selection-tools/sizing-selection-tools.html#belimo-hydronic-simulator, accessed October 2022

[3] *R. Petitjean*, „Total hydronic balancing: a handbook for design and troubleshooting of hydronic HVAC systems", Tour & Andersson Hydronics AB, Ljung, Sweden, 1994

[4] *** STAD_PN25_EN_low.pdf, https://www.imi-hydronic.com/product/stad-pn-25, accessed October 2022

[5] *P. Fridmann*, „Equilibrage thermohydraulique des installations de chauffage", Les éditions parisiennes (EDIPA), Paris, 1989

The importance of the correct determination of the input parameters in the FDS software; the importance of validating numerical studies with experimental studies

Importanța determinării corecte a parametrilor de intrare în software-ul FDS; importanţa validării studiilor numerice cu studii experimentale

Marius Dorin Lulea[1]

[1] doctor in civil engineering and installations
Technical University of Constructions from Bucharest, Romania
124 Lacul Tei Boulevard
E-mail: luleamariusdorin@gmail.com

Abstract
FDS is the software researchers use to simulate the evolution of a fire inside the buildings or to simulate exterior fires. FDS was used in research on modelling of the fire inside a room with dimensions of 3(m) x 6(m) x 2.7(m). The research included an experimental study and a computer modelling component to expand the probable scenarios. The research concludes that the FDS software can allow proper modelling of fire evolution, but an important stage is a phase of determining the model and calibrating it. Entering the input data correctly is an extremely important step.

Keywords:
FDS, CFD, fire, temperature, construction

Introduction

During the lifetime of construction, it can be charged with normal current loads (for example, the own weight of the construction, the weight of users, the weight of furniture or other stored materials, the action of the wind, the action of the weight of snow) or it can be submitted to exceptional loads but with high intensity (i.e. seismic action, fire action).

Designers must consider all likely situations when conforming a building and designing the construction to standards.

A current concern of construction designers is to simulate the action of fires and how a fire evolves inside a building. The international trend is to offer a more realistic representation of the evolution of the fire, not only in the design phase but also in the expertise phase of a fire that has already occurred.

Nowadays, fire modeling methods can be divided into three broad categories: simple methods, zonal methods, and complex methods (Figure 1).
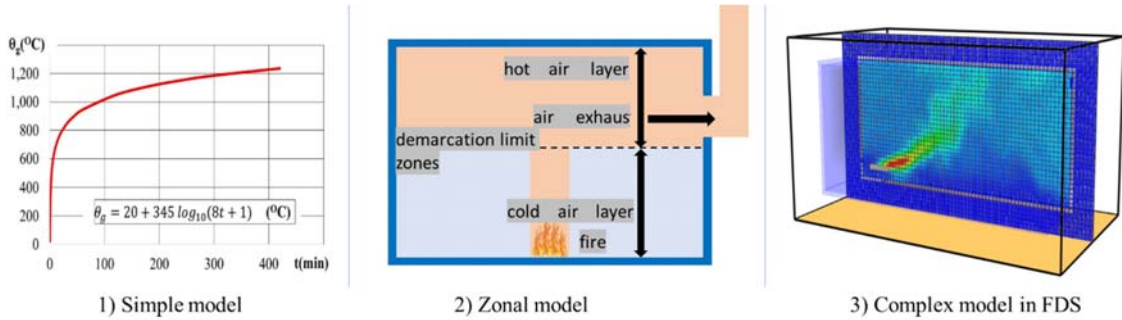
Figure 1 Types of models for describing fire action

Simple methods involve simple mathematical formulas, for example, the characterization of the space by the specific heat load. Zonal methods assume the division of spaces into two parts, the upper one with warm air and the lower one with cold air, each zone characterized by an average temperature and the height of the air layer. Complex methods involve modeling the fire as realistically as possible by solving complex equations describing fluid motion (CFD).

Areas covered

This opinion refers to the field of fire safety of constructions, being useful to building designers and researchers who use FDS in their studies.

This opinion refers to the importance of correctly establishing the input data in the FDS, this stage having extraordinarily large consequences for the results obtained.

Experiment

The research involved three main stages: carrying out the experiment, establishing the model and validating it, and carrying out numerical studies.

The experiment consisted in studying the internal temperature evolution inside a stand with dimensions of 3(m) x 6(m) x 2.7(m) (Figure 2).
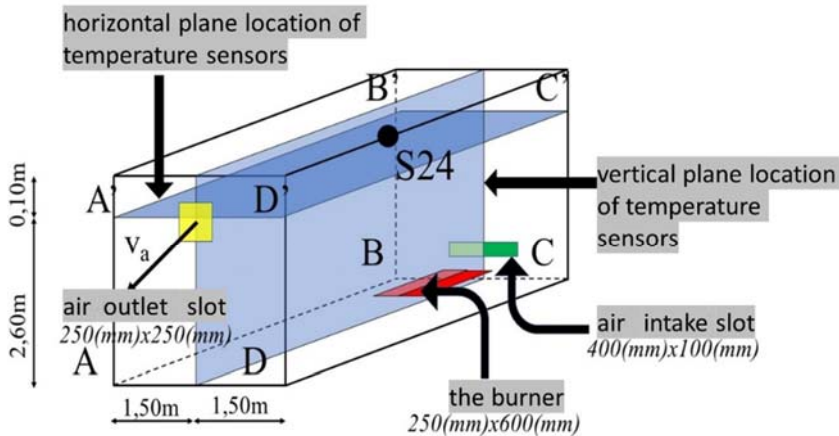
Figure 2 The experimental stand

Several K-type thermocouple sensors were mounted inside the stand, which recorded the interior temperature with the help of an ALMEMO data center.

The duration of data recording was 760 (s).

During the experiment, indoor temperatures rose from 20($^{\circ}$C) and exceeded 100($^{\circ}$C).

The heat source was represented by a burner that used LPG as fuel.

The evolution of interior temperatures at a given point during several experiments was recorded. The sensor was mounted almost centrally at the top of the stand, in the hot air area, where the sprinklers are usually located (sensor S24 from Figure 2).

Model setting and model validation

To be able to extend the research to hundreds of probable cases and to temperature ranges that cannot be safely reached with the help of an experiment, a mathematical model was made using the FDS software.

The modeling involved two main components: the establishment of the geometric characteristics and the establishment of the physical and chemical characteristics of the materials.

The geometrical characteristics of the components and their placement in space were achieved by direct measurement. This is about wall placement, hot air vents and cool air vents for compensation, fan placement, burner placement, and dimensions.

Physico-chemical characteristics imposed the need to determine the density of materials, thermal conductivity, specific heat, and other characteristics. Most of them were taken from product brochures, specialized literature, or other similar research.

Special attention was paid to the thermal conductivity of the outer walls of the experimental stand. The heat losses from inside the stand to the outside of the stand depending on the correct setting of the thermal conductivity.

The external components of the stand are the outer walls, the upper floor, the lower floor, the window that provides direct visual supervision of the experimental stand, and the door that provides access to the interior. To simplify the model, all these components with different thermal conductivities were not considered, but an equivalent thermal conductivity was established (Figure 3). The equivalent thermal conductivity also had to take into account the existing thermal bridges and the thermal conductivities of the actual components.
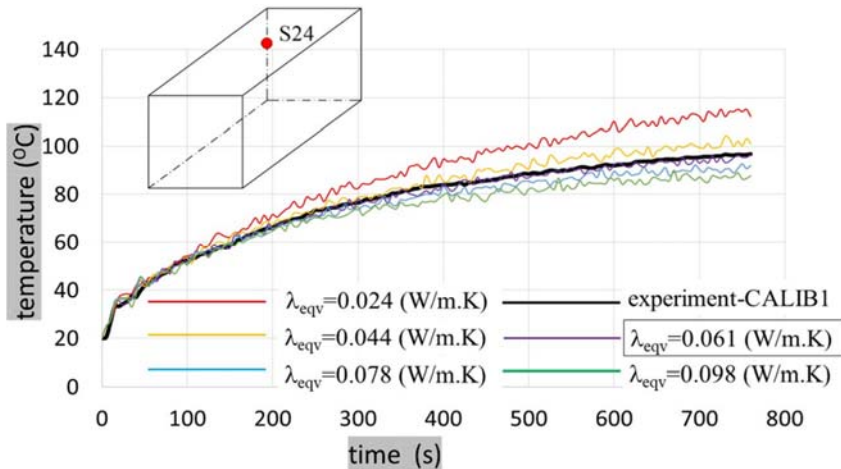
Figure 3 Temperature evolution graph at different values of the equivalent thermal conductivity

The equivalent thermal conductivity was established by successive iterations using FDS at different values until the deviations between the experimental indoor temperature records and those obtained from numerical modeling became minimal.

Conclusions
The FDS software is an extremely useful software tool in fire simulation and with very close to real results if the model is set up correctly.

It has been found that the correct determination of thermal conductivity has particular importance. Seemingly minor changes in these values lead to significantly different results. Taking the physico-chemical characteristics from the technical leaflets of the products used can lead to important errors.

Extending this observation to other input parameters, we can safely say that errors can accumulate, and this leads to significantly different output data.

If the analysis duration is longer, the accumulation of errors will become exponential, so at higher durations, it is necessary to use values as precise as possible and validated with more experimental results.

It is very important to use as many decimal places as possible. The level of detail can be established depending on the specifics of the study.

The validation of numerical studies with the help of experimental studies will certainly lead to a significant increase in the quality and correctness of the research.

Considerations regarding access to gas from renewable sources to the network existing gas distribution

Consideraţii privind accesul gazelor din surse regenerabile la reţeaua de distribuţie a gazelor naturale existentă

Diana Laura Merţan

Universitatea Politehnica Timişoara,
Facultatea de Construcţii, Departamentul Inginerie Civilă şi Instalaţii
2 Traian Lalescu Street, Timişoara, Romania
E-mail: mertan.diana@yahoo.com

Rezumat. *Consumul mondial în continuă creştere de gaze naturale şi rapiditatea epuizării rezervelor de combustibili fosili au tras un semnal de alarmă specialiştilor preocupaţi de căutarea unor soluţii energetice care să răspundă nevoilor actuale, pentru o creştere economică sustenabilă. Lucrarea de faţă prezintă accesul biometanului în sistemele existente de distribuţie a gazelor naturale, cu scopul diminuării consumului de combustibili fosili. Acest articol investighează indicatori specifici pieţei de gaze naturale din România, având drept ţintă identificarea unei soluţii eficiente privind suplimentarea de combustibili mai puţini nocivi decât combustibilii fosili, biometanul fiind o alternativă regenerabilă la combustibilii fosili. În acest caz, gazul „verde" - biometanul ajunge la utilizatorii finali prin intermediul conductelor de distribuţie existente.*

Cuvinte cheie: gaze naturale, energie regenerabilă, biometan, sistem distribuţie, sustenabilitate

Abstract. *The ever-increasing global consumption of natural gas and the rapid depletion of fossil fuel reserves have sounded the alarm to those concerned with finding energy solutions that meet current needs for sustainable economic growth. This paper presents the access of biomethane in existing natural gas distribution systems, in order to reduce the consumption of fossil fuels. This article investigates specific indicators of the Romanian natural gas market, aiming to identify an efficient solution for supplementing less harmful fuels than fossil fuels, biomethane being a renewable alternative to fossil fuels. In this case, the „green" gas - biomethane reaches the end users through the existing distribution pipes.*

Key words: natural gas, renewable energy, biomethane, distribution system, sustainability

1. Introduction

In the current environment, energy from renewable sources has been growing timidly, currently representing about 2% of total national energy production, the top ranking is still led by conventional non-renewable energy sources (coal, oil and natural gas) and non-conventional non-renewable energy sources (nuclear energy).However, with Romania's adherence to the European Green Deal (the Green Deal), the proportion of energy production from renewable sources should increase until 2030, so contributing to the creation of an energy strategy based on reducing dependence on imports, both at national and European Union level.

In order to achieve these objectives, the natural gas sector is going through a multitude of legislative changes today. Along with the other signatory states, Romania will have to create an intelligent natural gas distribution system and implement the mixture of natural gas with „green" gas in the existing pipeline system to facilitate the transition to clean energy. Other legislative objectives are found in the "Fit for 55" package: reducing energy poverty, increasing production from renewable sources and combating climate change. [1]

A development of the energy sector can only be implemented keeping in account the objectives of sustainability. To facilitate the transition to „green" energy, the International Energy Agency affirms that methane emissions coming from fossil fuels should be reduced by 45% until 2030. If this objective is achieved, global warming could be reduced by 0.3°C by 2040[2].

2. The current state regarding fossil fuels

To facilitate the application of sustainability strategies in the energy sector, the attention will focus on the process of forming the energy mix to reduce the use of fossil fuels. The way in which we can contribute is through the procedure of injecting renewable gases into the distribution networks.

Regarding to the identification of the way in which we can implement the objectives of sustainability to reduce the consumption of fossil fuels, firstly the composition of natural gases will be presented, then the procedure for determining the amount of energy consumed.

Since natural gas is part of the category of fossil fuels, the development of the energy sector is done by protecting the environment, using other types of sources, among which renewable sources are considered. [3]

Examining the composition of natural gases (Table 1), methane (CH_4) is identified as the principal component, to which is added the mixture of heavy hydrocarbons (butane, ethane, propane, carbon dioxide, nitrogen, hexane plus and pentane). Along with these, minor components are recorded in the chemical composition of natural gases: carbon monoxide (CO), nitrogen (N_2), hydrogen (H_2), oxygen (O_2), helium (He) as well as traces of constituents originating from sulfur. [4]

Minimum quality requirements necessary for the transport of natural gas and biomethane through pipelines related to the molar concentration, denoted wich Ci; Principal constituents for natural gas, raw biogas and upgraded biogas (biomethane)

Minor and major percentage components					
Natural gases	C_i	Raw biogas	C_i	Enhanced biogas (biomethane)	C_i
methane (CH_4)	min. 85	methane (CH_4)	45-75	methane (CH_4)	min. 90
carbon dioxide (CO_2)	max. 8	carbon dioxide (CO_2)	30-40		
ethane (C_2H_6)	max. 10	oxygen (O_2)	max. 1		
butane (C_4H_{10})	max. 1,5	hydrogen sulphide (H_2S)	0,0025-0,0030 (25-30 ppm)		
propane (C_3H_8)	max. 3,5	ammonia (NH_3)	max. 0,01 (max. 25-30 ppm)		
azote (N)	max. 10	azote (N)	1-2		
pentane (C_5H_{12})	max. 0,5	siloxane (R_2SiO)	traces		
hexane (C_6H_{14})	max. 0,1	water (H_2O)	traces		

Methane is one of the component elements in the gas mixture which helps to form the burning process. Along with it, alkanes and inert gases are identified in the natural gas structure, which are transported in the distribution network in lower concentrations.

Following the burning process, heat is released through rapid oxidation of combustible substances. Reaction products are used to make the burning process happen, and combustion gases are produced when the fuels are burnt.

Through the process of determining the amount of energy consumed by the final user, it is possible to determine the contribution of each participant to the consumption of natural gas.

The calculation formula for determining the amount of energy consumed by final users when using equipment consuming gaseous combustibles is as follows[5]:

$$E = V_b \times PCS \quad (1)$$

In which: E - natural gas energy (kWh), effect of converting the amount of natural gas into energy units; V_b - the corrected volume, determined under reference conditions (m^3); PCS- the superior calorific value of natural gas (kWh/mc), determined at the combustion temperature of 15^0C, using chromatographs.

In order to determine the amount of energy consumed, the superior calorific power must be known (Table 2). The superior calorific power, also known as the heat of burning, is established by economic operators [6] and is a qualitative parameter, registering inflections depending on the place of origin (domestic production, import).

Superior calorific value for different types of gas

Nr. Crt.	Name	Gaseous fuel type	Unit	Value
Energy values - natural gas, methane, biogas and biomethane				
1	Superior calorific power (PCS)	natural gas	kWh/mc	10,46
2	Superior calorific power (PCS)	methane	kWh/mc	11,06
3	Superior calorific power (PCS)	biogas	kWh/mc	4,44-7,78
4	Superior calorific power (PCS)	biomethane	kWh/mc	6,75-9,41

From a theoretical point of view, calorific power (kJ/ m^3N) for gaseous fuels it is expressed as follows [13]:

$$PC=\sum_{i=0}^{n} \frac{P_i \cdot c_i}{100} \quad (2)$$

where:

P_i- the specific calorific value of the element i (kJ/m^3N); C_i- concentration of composition I (expressed as a percentage).

So, on the basis of a chromatographic analysis, it is possible to determine the superior calorific power calculated from the complete burning of one m^3 of combustible.

Starting from the latest national monitoring reports for the internal natural gas market [7] and calculating for the year 2021 the annual consumption of the final domestic user in Romania, the value of 20.34 kWh/user in 2021 resulted. Calculated for Europe, energy consumption from fossil fuels is 35.11 kWh/user in 2021 [8]. It is noted that Romania is below the average threshold of energy consumption from fossil fuels.

3. Fuel gas - compatibilities

A way in which we can participate in the EU's common action on harnessing renewable gas is to inject it into existing pipelines. Thus, it is necessary to establish the compatibility conditions between these types of gases and the non-renewable ones. It should be emphasized that there is a European Standard in the works that tries to constitute a common norm regarding the technical conditions that must be respected for the contribution to the energy mix of biomethane [9]. Among the technical conditions that will be agreed by the signatory states (currently 17) are, among others: the determination of the Wobbe index and the calorific power, conditions that differ according to each country.

Both Romania and the rest of the EU member states have identified a way to combat the current energy crisis, having to establish certain common quality criteria that define gases.

Researching the national energy sector, we found that there is potential to supplement a certain amount of biomethane, derived from biogas, in natural gas distribution pipelines.

Biogas is obtained through biotechnological operations, involving the process of anaerobic fermentation made from the degradation of organic matter. Through the technological process of biogas treatment, biomethane is obtained, which is part of the category of renewable gases.

A characteristic that needs to be highlighted is the difference between biogas and natural gas in terms of chemical compositions (Table 1). The main component of the gas mixture is methane, which contributes rapidly to the increase in greenhouse gas emissions, in contrast to biomethane, which can be obtained through sustainable methods. Along with it, among the chemical compounds we also list: carbon dioxide (CO_2), hydrogen (H_2), but they can also include certain impurities [10]. By means of the innovative techniques used to eliminate the harmful constituents that are part of the biogas composition (H_2S, CO_2, siloxanes), the following are listed: the absorption process, which includes chemical or physical absorption; the adsorption process (adsorption by pressure and temperature variation), the vacuum technique, the membrane separation method, the cryogenic separation method, the carbon capture and storage method and the use of hybrid technologies [11].

From the point view of compatibility conditions for the existing natural gas network, biogas is a key element to reduce dependence on imports. However, in this case, through the biogas purification process, the aim is to eliminate the existing CO_2 content of 30-40% and remove other contaminants such as: water vapor, hydrogen sulphide (H_2S), oxygen (O_2), nitrogen (N), ammonia (NH_3), siloxane (R_2SiO) and dust particles, with the aim of obtaining biomethane, which has qualities similar to natural gas. Biogas contains between 45-75% methane (CH_4), and to improve energy efficiency, the methane content will be increased by reaching the minimum quality threshold (Table 1) [11].

In the context of harmonizing national legislation with regulations issued at the EU level, it is necessary to establish the Wobbe index, to determine the reference threshold for the superior calorific power, establish the temperature by reference to standard reference conditions. All this is necessary to achieve compatibility between the two types of combustible gases used [10].

The Wobbe index (expressed in MJ/m^3) is defined as follows [13]:

$$I_w = \frac{PCS}{\sqrt{G_S}}, \quad (3)$$

where:

PCS –superior calorific power, expressed in MJ/m^3; G_s – specific gravity, expressed in N/m^3.

The Wobbe index represents one of the technical indicators characteristic of fuel gases, being defined as an indicator for their interchangeability. Fig. 1 inserts the recommended energy values for the Wobbe index specific to natural gas and methane compared to biomethane. Thus, the recommendations for harmonizing the legislation

on unitary standardization, with the implications of the signatory member states, regarding biomethane for injection into natural gas distribution pipelines were taken into account [13].
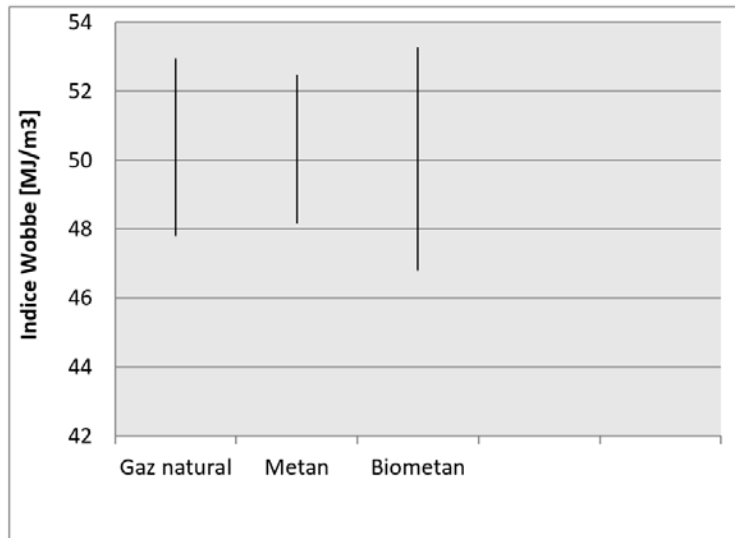
Fig. 1. Representative Wobbe index for natural gas, biomethane and methane

Due to the high concentration of CO_2 existing in the raw biogas, the calorific power is implicitly influenced. The biogas treatment process aims to capture and store the CO_2 content (as well as other contaminants) in order to obtain biomethane that will acquire superior characteristics.

Combustible gases obtained through biological processes have a low calorific power, approximately 4.44-7.78 kWh/mc, but following the elimination of the CO_2 concentration, as well as the removal of other specified contaminants listed, an increase in the methane content will be recorded above 90 %. It is known that the PCS for biogas is between 4.44-7.78 kWh/mc, respectively 45-75% methane. The PCS for biomethane is calculated, considering that the improved biogas contains 98% methane, then the PCS of biomethane will be between 6.75-9.41 kWh/mc, the PCS being influenced by the raw material used.

4. Conclusions

In the present article we have created an overview for the possibility of introducing biomethane into the existing natural gas networks. There is a need to ensure a source of renewable fuel energy to complement the natural gas in the distribution system, namely biomethane.

Romania's economy could have problems if only fossil fuels were consumed. The consumption can be covered by supplementing with biomethane in the existing natural gas distribution networks, taking into account the Wobbe index that must be

respected, appreciating that the necessary biomethane could be obtained from the recovery of organic waste.

Naturally, the demand for natural gas will increase, the competition on the gas market will also increase. Existing networks will be extended and interconnected with those of EU member states, having a positive influence on improving energy security. Romania must target for a technological development aimed at the use of „green" gases, in order to reduce the consumption of fossil fuels.

Some different approaches to the EU regulations for creating an intelligent natural gas distribution system that include „green" gases persist today, not being applicable in Romanian legislation. The verification of the specialized literature shows the need to establish the influential key index for determining the compatibility of the two types of fuel gas as a basis for the development of the future method by injecting biomethane into the existing systems, thus reducing the consumption of natural gas. The overall conclusion is that the influential indicator chosen for gas interchangeability highlighted in this paper helps research and development of mixed gas systems, determining consumption analysis methods and reducing fossil fuels used. This response to current needs ensures sustainable economic growth for all natural gas consumers.

Reference

[1] Council of the European Union, Overview of progress of the "Fit for 55" package of legislative proposals, Brussels, 2021.

[2] European Parliament Resolution, European Union Strategy to Reduce Methane Emissions2021/2006(INI), European Commission, 2021.

[3] Khaled O., Mohammad A. A., Tabbi W., Khaled E., Enas T. S., Hussein M. M., Olabi A.G., „Biogas role in achievement of the sustainable development goals: Evaluation, Challenges, and Guidelines", Elsevier, 2021, pag. 1-16.

[4] Faramawy S., Zaki T., Sakr A.A.-E., „Natural gas origin, composition, and processing: A review", Journal of Natural Gas Science and Engineering, 2016, pag. 35-48.

[5] The regulation for measuring the quantities of natural gas traded in Romania, approved by order of President of A.N.R.E.no. 62/2008, year 2008

[6] https://delgaz.ro/putere-calorifica-superioara, accessedJune 2022.

[7] A.N.R.E monthly monitoring reports for the internal natural gas market, year 2021.

[8] Report Energy on European Gas Markets with focus on the European barriers in retail gas markets Q1-Q3, Market Observatory for Energy, 2021.

[9] Dr Wellinger A., „European biomethane standards for grid injection and vehicle fuel", Conference, Brussels, 2017, coroborat cu M/475 Mandate to CEN for standards for biomethane for use in transport and injection in natural gas piplines, Brussels, 2010.

[10] Yaqian Z., Ange N., Doan P., Nathalie L., „A Review of Biogas Utilisation, Purification and Upgrading Technologies – review", Springer Science, 2016, pag. 1-4.

[11] Babak A., Sara B., Somchai W., Mostafa S. S., „A review of recent progress in biogas upgrading: With emphasis on carbon capture", Elsevier-Biomass and Bioenergy, 2022, pag. 1-21.

[12] Filipe M. Quintino, Nuno Nascimento, Edgar C. Fernandes, „Aspects of Hydrogen and Biomethane Introduction in Natural Gas Infrastructure and Equipment", MDPI-Hydrogen, 2021, pag. 1-18.

[13] The Wobbe Index in the H-gas standard and renewable gases in gas quality standardization, Presentation by CEN, Sector Forum Gas WG Pre-normative studies on H-gas quality parameter (SFGas GQS), Madrid Forum, 2021.

Biomechanical models used in the analysis of vibrations induced to the human organism

Modele biomecanice utilizate în analiza vibrațiilor induse organismului uman

Alexandru Toader[1], Cristian Pavel[2], Florin Bausic[2], Robert Ursache[3]

[1]-drd ing. Faculty of Mechanical Engineering and Robotics in Construction UTCB
59 Calea Plevnei, Bucharest, Romania

[2]-prof.univ.dr.ing. Faculty of Mechanical Engineering and Robotics in Construction UTCB
59 Calea Plevnei, Bucharest, Romania
E-mail: cristian.pavel@utcb.ro
E-mail: florin.bausic@utcb.ro

[3]-drd ing. Faculty of Mechanical Engineering and Robotics in Construction UTCB
59 Calea Plevnei, Bucharest, Romania
E-mail: robionut@gmail.com

Summary. An analysis of the biomechanical models associated with the human body is performed (from 1 degree of freedom to 4 degrees of freedom).
Following the analysis of the biomechanical models, the average frequencies found in different components of the human body are presented.

Abstract. This paper focus on biomechanical models analysis of human body from one to five degree of freedom. As result of this analysis the medium frequencies of different human body elements are found.

Key words: vibrations, human body, biomechanical models

INTRODUCTION

This article presents a synthesis of the biomechanical models associated with the human body from models with 1 degree of freedom to models with 16 degrees of freedom. After a detailed discussion of each biomechanical model, the document ends with a table in which the average frequencies found in different components of the human body are presented.

1. THE MODEL NOTION

The concept of a model has appeared since ancient times, initially being an attempt to represent, imitate and explain the environment through cave drawings.

Throughout the development of human civilization, fundamental concepts of elementary mechanics have been developed. These concepts were later developed and used in successfully describing the movements of the human body.

The fragility of the human being that also manifests itself in the case of exposure to vibratory phenomena has led to in-depth research in the area of determining and combating negative effects (causing occupational diseases) that vibrations have on the human body. The area of beneficial effects was not neglected either, although the research was of a smaller scale.

All these findings realize the importance of the biomechanical modeling of the human body subjected to the action of vibrations. Although it is rarely possible to check the results obtained on the basis of a model with those obtained from determinations on the real model, simulations on different models can be done to identify the optimal model.

Biomechanical models associated with the human body [30],[92], they underwent successive transformations that increased the complexity and accuracy of explaining the phenomena and processes that occur in the human body.

These models to be viable, must be found on the border between complexity and simplicity.

1.1.   The evolution of the biomechanical modeling concept over time

The concept of model has been used since ancient times, at the beginning being an attempt to represent, imitate and explain the environment.

As human civilization developed, fundamental concepts of elementary mechanics were defined. These notions were later developed and used to successfully describe the movements of the human body. In the following lines, some of the significant figures of history and the chronology of some of the most important discoveries and researches in this field are shown.

> ➢ Aristotle (384-322 B.C.) – he is the one who stated the first notions in treatises about the parts of animals and their movements in works such as ”De Partibus Animalium”, ”De Motu Animalium”, ”De Incessu Animalium”.
> ➢ Archimedes (287-212 B.C.) – discovers the principles of hydrostatics relative to the floating of bodies, still used today in the biomechanics of swimming, explained the law of levers and made studies on the center of mass.
> ➢ Heron of Alexandria (10-70 A.D.) – he carried out research on levers and is considered the father of the polytechnic school.
> ➢ Galen (131-201 A.D.) – studies movements, distinguishes between sensory and motor nerves, between agonist and antagonist muscles,

        describes muscle tone and introduces the terms diarthrosis and synarthrosis still used today in biomechanics.

- Pappus (290-350 A.D.) – define with precision the center of mass and describe some of its properties.
- Philoponus (490-570 A.D.) – is the one who brought up the concept of "inertia" for the first time.
- Leonardo da Vinci (1452-1519) – the famous Renaissance artist, studied most of the elements related to the mechanics and anatomy of the human body and the center of gravity. He described the action of synergistic muscles that participate in walking, jumping and running.
- William Harvey (1578-1657) – is considered to be the father of fluid biomechanics.
- Alfonso Borelli (1608-1679) – through his remarkable studies of biomechanics he showed that the bones and segments of the human body act like levers that are moved by muscles, according to some principles of classical mechanics.
- Giorgio Baglivo (1668-1706) – distinguishes for the first time between smooth and striated muscles. He shows that the former are responsible for sustained contractions and the latter for rapid movements.
- Nicolas Andry (1658 – 1742) – names and defines, right in the title of his work Orthopedia, the art of preventing and correcting the deformations of the child's body.
- Weber brothers – substantiates on scientific bases the research in the field of biomechanics started by Borelli.
- Jansen – using serial photographs to study the revolution movement of the planet Venus, proposes the same method for the study of the human body.
- E. Muybridge (1831-1904) – he is the first to succeed in motion capture, making the first serial photographs of the movement of a racehorse.
- Marey and Demeny – prints on the photographic plate the successive positions of a movement, obtaining the cyclogram of the movement.
- C. W. Braune (1831-1892) – his experiments and conclusions on movement and walking are still valid today.
- Julius Wolff (1836-1902) – formulated what is known as "Wolff's Law" which describes the relationship between mechanical influence and bone geometry. He considered that the modification of the internal structure and configuration of man is the result of the change of shape and function of the bones, in correspondence with the laws of mathematics.

The parameters characterizing a biomechanical system will depend on the type of model used. For a physical biomechanical system there are two general methods of approach, which lead to the determination of the parameters that characterize the dynamic behavior of the system, namely: the analytical method and the experimental method.

        These methods are shown schematically in the figure 1.1.

```
                    ┌─────────────────────┐
                    │  REAL BIOMECHANICAL │
                    │       SYSTEM        │
                    └─────────────────────┘
                               │
                               ▼
                    ┌─────────────────────┐
                    │     METHODS OF      │
                    │      APPROACH       │
                    └─────────────────────┘
```
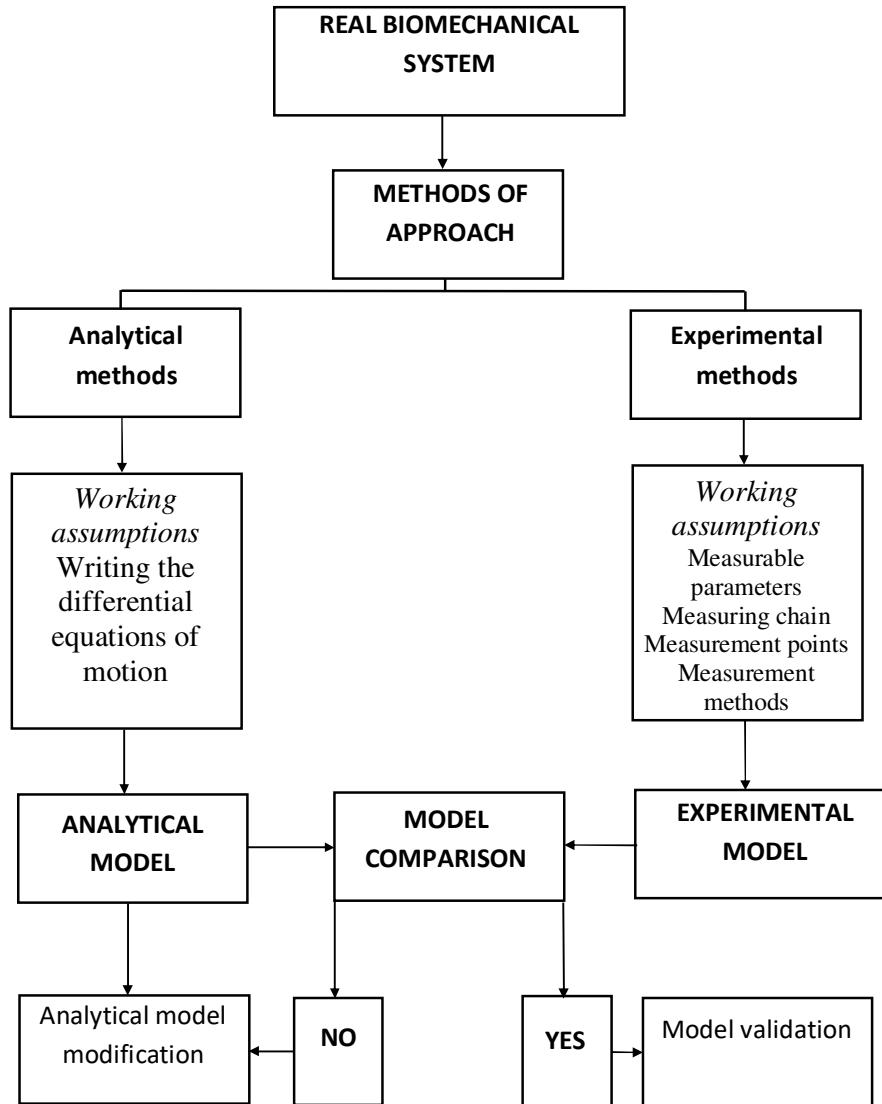
Fig. 1.1. General methods of approach to biomechanical systems [12],[17]

2. The human body – associated biomechanical models

The biodynamic study of humans can be traced back to 1918, when Hamilton (1918) investigated the effects of vibration on workers in limestone quarries. Many experimental evidences have shown that a human body can be injured by vibrations. Approximately 12 million workers in the US were reported to be affected by vibration (Amirouche, 1987), [7]. It is also well known that vibration can fracture the spine when subjected to strong vertical acceleration. In addition, the transmission of vibrations to the human body can reduce comfort or even have a negative effect on health. If the vibration is very severe, for example in an off-road vehicle, injuries to passengers and the driver can become a problem.

55

Research into the effects of vibration on seated workers indicated that the after-effects could be very harmful and in some cases lead to permanent injury (Kelsey and Hardy, 1975),[65]. Some results have suggested that low back pain is the result of continuous exposure to vibration (Pope et al., 1986),[101] and occurs more frequently among vehicle drivers than in representative control groups (Pope et al., 1987, [102]). As travel length increase, the driver is more exposed to vibrations that come mainly from the interaction between the road profile and the vehicle.

Therefore, in recent years people have become more concerned about vibrations and are looking for a more comfortable environment. In general, the study of biodynamic responses in humans can be classified into statistical (experimental) and analytical methods. According to different test subjects, the experimental study can be further classified into two groups.

In the study of mechanical injury to humans, animals (rats, pigs, etc.), human cadavers and mannequins are usually selected as test subjects to avoid injury to human beings. Cesari and Ramet (1982),[34], used impact tests to obtain the maximum fracture load on the pelvis and established pelvic injury criteria accordingly. Alem et al. (1984),[4], performed axial impact tests on 19 human cadavers to study the mechanical properties of the head-neck-vertebral structure and defined the injury standard.

Pintar and Yoganandan (1989),[99], embedded six axial load sensors in and on the skin of seven cadavers to study the biodynamic and anatomical responses of the neck and cervical spine. Bohman et al. (2000),[22], implemented a series of tests using the Hybrid III 50% manikin to investigate the influence of the restraint system on neck loads in frontal impacts.

In addition, Yoganandan et al. (2000),[133], studied the biomechanical studies of one male and four female human cadaver in rear impact situations. Therefore, the forces and moments in occipital conditions were evaluated but also the risks of neck injury.

In an effort to define general values to characterize the biodynamic response of the seated body in the most commonly encountered work environments, Boileau et al. (1998),[22],[23] identified seat-to-head transmissibility (STH), driving point mechanical impedance (DPM) and apparent mass (AP) from prevailing published data by synthesizing and creating envelopes of different sets of selected dates. Those values of the various biodynamic response functions are defined for subjects maintaining an upright sitting posture without backrest support, with the feet resting on a vibrating platform.

Table 1.

One- and two-degree-of-freedom lumped parameter models of seated human subjects

Author	Biomechanical parameters			Remarks	Schematic of the model
	Mass (kg)	Damping (N-s/m)	Stiffness (N/m)		
Coermann model – one degree of freedom (1962)	m_1 56.8 ± 9.4	c_1 3840.0 ± 1007.0	k_1 75 500.0 ± 28 300.00	• Linear model – one degree of freedom • Total weight 56.8 kg • Excitation: $\ddot{z} = 5\sin\omega t$	
Wei and Griffin (1998)	m_1 43.4	c_1 1485.0	k_1 44130.0	• Linear model – one degree of freedom • Total weight 51.2 kg • m_0 in rigid contact with the seat • Excitation: $\ddot{z} = 5\sin\omega t$	
Model with two degrees of freedom Muksian and Nash (1976)	m_1 7.8	c_0 -	k_0 -	• Non linear model – two degrees of freedom • Total weight 79.83 kg • $c_1' = 17289 f_0^2$, f_0 (excitation frequency) 10Hz • 0, otherwise • m_0 in rigid contact with the seat • Excitation: $\ddot{z} = 5\sin\omega t$	
	m_2 5.44	c_2 686.0	k_2 0.0		
	m_1 47.17	c_1' See note c_1 467.0	k_1 63318.0		
	m_0 27.22	c_0 1780.0	$k0$ 27158.0		
Alken (1978)	m_2 5.5 ± 0.9	c_2 318.0 ± 161.0	k_2 41 000.0 ± 24 100.00	• Linear model – two degrees of freedom • Total weigth 56.8 kg • Excitation: $\ddot{z} = 5\sin\omega t$	
Wei and Griffin (1998)	m_1 51.3 ± 8.5	c_1 2807.0 ± 1007.0	k_1 74 300.0 ± 17400.00		

3.15	m_2	c_2	k_2
	10.7	458.0	38 374.0

- Linear model – two degrees of freedom
- Total weight 50.8 kg
- m_0 in rigid contact with the seat
- Excitation: $\ddot{z} = 5 \sin \omega t$

	m_1	c_1	k_1
	33.4	761.0	35 776.0
	m_0	c_0	k_0
	6.7	-	-

Three-degree-of-freedom lumped parameter models of seated human subjects

Author	Biomechanical parameters			Remarks	Schematic of the model
	Mass (kg)	Damping (N-s/m)	Stiffness (N/m)		
Model with three degrees of freedom Suggs, etc. (1969)	m_3 5.5 ± 0.9	c_3 318.0 ± 42.0	k_3 74 300.0 ± 17 400	• Linear model – three degrees of freedom • Total weight 56.8 kg • Masses m_1 and m_2 it connects rigidly because the values of k_2 and c_2 are infinite • Excitation: $\ddot{z} = 5 \sin \omega t$	
	m_2 36.0 ± 6.0	c_2 ∞	k_2 ∞		
	m_1 15.3 ± 2.5	c_1 2806.0 ± 1000.0	k_1 40 900 ± 22 700		

Conclusions

Lumped parameter models from the literature were also analyzed and validated in what by synthesizing different experimental data. The following conclusions can be drawn from the above:

1. Lumped parameter models are limited to univariate analysis. These mathematical models include linear and non-linear systems with varying degrees of complexity depending on the objective of the analysis

2. From the analysis of biomechanical models: with one degree of freedom Dieckmann (1957) (Coermann, 1962), two degrees of freedom (Wei and Griffin, 1998), (Allen, 1978), (Muksian and Nash, 1976), with three degrees of freedom (Suggs et al., 1969), (Allen, 1978), (Cho-Chung Liang, Chi-Feng Chiang, 2006 and Suggs C.W., Abrams C.F., Stikeleather L.F., 1969), (A. Picu 2009), with four degrees of freedom (Wan and Schimmels, 1995), (1998, Liu, Shi), (Boileau and Rakheja,

1998), Wagner and Liu (2000), with six degrees of freedom (Muksian and Nash, 1974), with seven degrees of freedom (Patil et al., 1977), (Cho-Chung Liang, Chi-Feng Chiang, 2005 and Patil, M.K., Palanichamy, M.S., Ghista, D.N., 1977), (Abbas et al., 2010), (Sengkang et al., 2013), with nine two-dimensional degrees of freedom (Harsha et al., 2014), with eleven degrees of freedom (Qassem et al., 1994; Qassem and Othman, 1996), the important frequencies of the body components result human presented in table 18., page 110, [82] namely:

Head - 2.06 Hz; chest - 1.2 Hz; trunk - 1.21 Hz, forearm - 1.17 Hz, arm - 3.39 Hz, thigh - 4.7 Hz, foot - 0.93 Hz.

3. From the analysis of the results of the biodynamic models presented in [100], the conclusion that will be used in the validation of the biodynamic models with the results of experimental measurements is drawn, the important frequencies of the component parts of the human body are those in the table below, table 4.7., [82].

Table 4.3.

The important frequencies of the human body [82]

Name of component part of the human body	Frequency [Hz]
Head	2,06
Chest	1,20
Trunk	1,21
Forearm	1,17
Arm	3,39
Thigh	4,7
Leg	0,93

Selective Bibliography

[1] Bausic Florin, **Toader Daniel**, Bausic Alexandra, Toader Eliza – „Contribuții privind analiza modelelor biomecanice ale organismului uman supus acțiunii vibrațiilor" – Sinteze de Mecanica Teoretica si Aplicata, Volumul 8 (anul 2017), Numarul 3 – Matrix Rom

[2] Bausic Florin, **Toader Daniel**, Bausic Alexandra – „Metodă și dispozitiv pentru monitorizarea în timp real a corpului uman supus acțiunii vibrațiilor" – Sinteze de Mecanica Teoretica si Aplicata, Volumul 9 (2018), Numarul 3 – Matrix Rom

[4] Bausic Florin, **Toader Daniel**, Bausic Alexandra, Bacanu Sorana – „Contribuții privind analiza vibrațiilor induse organismului uman în timpul procesului de lucru" – Sinteze de Mecanica Teoretica si Aplicata, Volumul 10 (anul 2020), Numarul 1, pag , 57-60, ISSN 2068-6331 – Matrix Rom

[5] **Toader Daniel**, Alexandra BAUȘIC, Florin BAUȘIC - Analiza experimentală a vibrațiilor induse organismului uman- Sinteze de Mecanica Teoretica si Aplicata, Volumul 11 (anul 2020), Nr.l 2,pag 109-112, – ISSN 2068-6331 Matrix Rom

[6] **Toader Daniel**, Dogaru Marina, Ursache Robert, Bausic Florin – „Partial experimental contributions of the validation of biomechanical models of the human body subjected to the action of mechanichal vibrations – Modelling in Civil and Environmental Engineering, Scientific Journal, Vol. 16 - No.4: 25-33-2021, Doi: 10.2478/mcee-2021-0018, ISSN 2784-1391, Tehnical University of Civil Engineering Bucharest

[7] Legendi, A., Bauşic, F., Pavel, C. - Analiza transmisibilităţii vibraţiilor utilizate în scop terapeutic-metoda de investigaţie a structurii osoase, SIMEC 2007, 31 martie 2007, Editura Conspress Bucureşti, ISBN 973-7797-83-3, pag. 133-136;

[8] Panaitescu-Liess, R. - Modele biomecanice asociate organismului uman. Stadiul actual al cercetărilor – Raport de cercetare, februarie 2012;

[9] Reynolds, D.D. and Soedel W. (1972) Dynamic Response of the hand-arm system to a sinusoidal input. Journal ofSound& Vibration 21,339-353

[10] Miwa, T., Y. Yonekawa Y., Nara A,,.Kanada K., Baba K. (1979) - Industrial Health17,85-122 Vibration isolators for portable vibrating tool . Part-1. Agrinder.

[11] Mishow JW, Suggs C.W., (1977) - Hand-arm vibration part-1, vibration response to the human hand. Jr. of Sound and Vibration 1977,53; 545-58

[12] Meltzer G. (1979) - Proceedings of the International Symposium on Man under Vibration Suffering and Protection, Udine, Italy, 210-221. A vibration model for the human hand-arm system